Critical Review of Electro-kinetic Remediation of Contaminated Soils and Sediments: Mechanisms, Performances and Technologies

Ding Han · Xingyi Wu · Rui Li · Xianqiang Tang · Shangbin Xiao · Miklas Scholz

Abstract Remediation of contaminated soil and sediment is important for improving the eco-environmental quality. Electro-kinetic remediation (EKR) is an environmentally friendly technology to migrate and remove pollutants from the soil and sediment matrix. This paper analyses the mechanism and performance of EKR of heavy metals, organic pollutants, and compound pollutants. Moreover, the effect of optimizing individual EKR through soil and sediment pre-treatment (adding acid/oxidant/co-solvent/surfactant, stirring, heating, etc.), electrode optimization (exchange electrode, anode approximation, electrode matrix, etc.), and applying multi-technology combination (electro-kinetic permeable reaction barrier/Fenton/ion, exchange membrane/ ultrasonic/electrolyte enhancement, etc.) was evaluated. Factors including incomplete separation of pollutants, variation in physico-chemical properties and microstructure of soil/sediment, and difficulties in in situ practice have restrained the field application of EKR. To solve the above technical challenge, an integrated EKR technology based on pollutant in situ separation, followed by separated contaminant treatment, and subsequent valuable elements recovery is proposed.

D. Han · X. Wu · S. Xiao
College of Hydraulic & Environmental Department, China Three Gorges University, Yichang 443002, China

D. Han · X. Wu · R. Li · X. Tang
Basin Water Environment Department, Changjiang River Scientific Research Institute, Wuhan 430010, China

R. Li · X. Tang (✉)
Key Lab of Basin Water Resource and Eco-environmental Science in Hubei Province Changjiang River Scientific Research Institute, Wuhan 430010, China
e-mail: ckyshj@126.com

M. Scholz (✉)
Division of Water Resources Engineering, Faculty of Engineering, Lund University, P.O. Box 118, 22100 Lund, Sweden
e-mail: miklas.scholz@tvrl.lth.se

M. Scholz
Department of Civil Engineering Science, School of Civil Engineering and the Built Environment, University of Johannesburg, Kingsway Campus, PO Box 524, Aukland Park, Johannesburg 2006, South Africa

M. Scholz
Department of Town Planning, Engineering Networks and Systems, South Ural State University (National Research University), 76, Lenin prospekt, Chelyabinsk 454080, Russian Federation

M. Scholz
Institute of Environmental Engineering, Wroclaw University of Environmental and Life Sciences, ul. Norwida 25, 50-375 Wrocław, Poland

1 Soil and Sediment Treatment by Electro-kinetic Remediation

Mining, electroplating, and other industrial activities, as well as sewage irrigation, the use of chemical fertilizers, and other agricultural production processes, lead to large amounts of heavy metals and organic pollutants accumulating in the soil and/or sediment. These pollutants can bio-accumulate in living organisms and cause a threat to the health of plants and animals including humans (Forstner, 2004; Li et al., 2018).

Soil and sediment pollution has become a global environmental crisis. A variety of remediation technologies have been developed for soil and sediment pollution, including solidification-stabilization, phytoremediation, and leaching. However, these methods have certain limitations in their application scope. For example, in bioremediation, the mobility of microorganisms in soil is poor. Organisms are easily inhibited by the toxic effect of pollutants. In phytoremediation, the absorption and accumulation of pollutants by hyperaccumulators are very slow, and the remediation time is often too long for practical purposes. Leaching requires higher soil permeability, and the legacy of a leaching agent may cause secondary pollution. In addition, in the process of remediation, due to the comprehensive influence of different pollutant properties and soil characteristics, it is difficult for the aforementioned remediation technology to quickly and effectively remediate contaminated soil with low permeability. In such a case, electric remediation technology has received more attention.

EKR is a technology for migration, separation, and removal of pollutants in soil and sediment under an electric field, which is cost-efficient and has low environmental impacts (Vocciante et al., 2017). Casagrande (1948) firstly tested the principle of electroosmosis on real soil in the field, and consolidated soft clays by employing an electric current. In the early days, the technology was mainly used for sediment dehydration as well as strengthening of foundations (Micic et al., 2001). During the late 1980s, directional migration of ions in the electric field was first discovered within the process of electric dehydration, and the application of the EKR concept to remove heavy metals from contaminated soil was proposed in 1992 (Lindgren et al., 1994). Subsequent experiments have, for example, confirmed that between 85 and 95% of phenol can be removed from saturated kaolin when EKR is applied (Acar et al.,

1992). Over the last few decades, EKR has been widely used in the removal of a variety of pollutants including heavy metals such as Cu, Pb, Zn, and Cd (Al-Hamdan & Reddy, 2008; Ferro et al., 2014); organic pollutants including phenanthrene, thorium, triclosan, aniline, and phenol (Chung & Kamon, 2005; Li et al., 2000; Ricart et al., 2008); salts such as fluorine, nitrate, and phosphorus (Kim et al., 2012; Lee et al., 2011; Tang et al., 2020; Zhou et al., 2014; Zhu et al., 2009); and radioactive substances such as uranium (Mao & Pan, 2015; Xiao et al., 2020).

Using two or more remediation methods at the same time to form a joint remediation system can not only improve the remediation rate and efficiency of single contaminated soil, but also overcome the limitations of single remediation technologies. Permeable reaction walls, electric Fenton, phytoremediation, and ultrasound (Cang et al., 2011; Fernández de Dios et al., 2014; Mumford et al., 2015; O'Connor et al., 2003; Pham et al., 2009) have been integrated into EKR technology.

At present, laboratory work progress linked to EKR technology has been considerable, but it still has great difficulties to overcome in engineering practice. There are still some technical problems to be solved, among which the most important challenges include pH control at both sides of the electrode, the "polarization effect," and the "focusing effect" (to be described in more detail in the second part).

2 Mechanisms and Models to Understand Electro-kinetic Remediation

2.1 Mechanisms

EKR achieves the purpose of remediation by applying an electric field to the contaminated soil/sediment, enriching the pollutants to the cathode or anode zone through electroosmosis, electromigration, and electrophoresis (Fig. 1). Electric migration is the movement of charged dissolved ions through an aqueous medium toward the electrode with a polarity opposite the ion charge (Wang et al., 2021). Electro-osmosis is the movement of pore fluid and dissolved constituents within a porous medium that typically occurs between the anode and cathode, because of the negative charge characteristic of the soil particle surface (Cameselle & Reddy, 2013). However, the change of surface charge of soil may change the direction of electroosmosis.
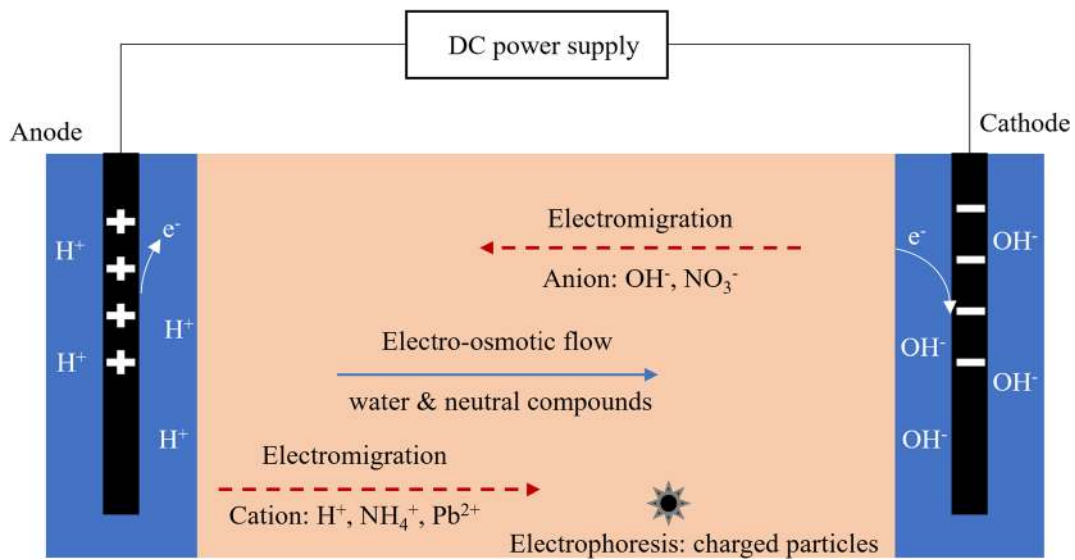
Fig. 1 Schematic diagram of (a) the electro-kinetic remediation principle (DC, direct current); and (b) comparison of electroosmotic flow in a single capillary

Electrophoresis refers to the transport of charged particles or colloids in soil under the action of an electric field. Soil organic matter, microbial cells, and small soil particles are colloids, and when heavy metals and other pollutants are adsorbed on the surface of colloid or charged particles, they will be discharged together. However, the effect of electrophoresis can be ignored, because of the low mobility of charged soil particles in the process of electric remediation. Therefore, the actual migration speed of heavy metal ions in soil pore water is determined by the action of electric migration and electroosmosis under the action of an external direct current electric field.

In the electro-kinetic remediation process, the liquid phase mass transfer of pollutants is mainly realized through four processes: electromigration, electroosmotic flow, convection, and diffusion (Acar et al., 1993). For EKR, electroosmosis and electromigration contribute most to the pollutant removal, while electrophoresis and electrochemical oxidation occurs only for some types of pollutants (Table 1). The most possible reason for this is that within the process of compacting the soil/sediment matrix, free movement of large colloidal particles is usually limited, while the dissolved pollutants in pore water migrate relatively easily (Reddy & Saichek, 2003). The migration rate and amount of ions are related to the porosity, ion charge, soil temperature, soil moisture, and voltage potential (Acar & Alshawabkeh, 1993).

Organic pollutants are electrically neutral in general, and the main mechanism for electrically removing organic pollutants from soil and sediment is
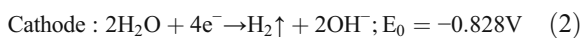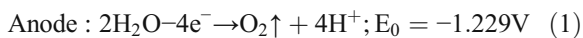
Table 1 Characteristics for electro-kinetic remediation treating different kinds of pollutants

Target pollutants		Pollutant properties	Dominant removal processes
Heavy metals	Cd, Pb, and Hg	Easily to form a precipitate with OH^- and low solubility	Electromigration and electroosmosis
Organic pollutants	PCB, PAH, and petroleum hydrocarbons	Low solubility, difficult to biodegrade, adsorbs to sediment particles and electrically neutral	Electroosmosis, electromigration (charged), and electrochemical oxidation
Inorganic ions	Nitrite, fluorine, radioactive species (Ur and Cs)	High solubility	Electromigration and electroosmosis
Mixed pollutants	Heavy metals and organic pollutants	Active interaction between pollutants	Electromigration and electroosmosis

electroosmosis (Alcántara et al., 2010). Acar et al. (1992) and Bruell et al. (1992) carried out experiments to remove phenol and hydrocarbons (benzene, toluene, and trichloroethylene) from kaolin and clay. They found that EKR can remove a certain amount of organic pollutants from fine soil particles by electroosmosis. However, the application of an electric field does not promote the dissolution and desorption of organic matter. For inorganic nutrients such as nitrate, electromigration dominates the removal process, and EKR can remove 90% of nitrate, and the residual nitrate ions in the soil are mainly concentrated near the anode (Manokararajah & Ranjan, 2005; Zhou et al., 2015).

For mixed pollutants, the interactions between different pollutants may occur when EKR is applied. EKR was performed with mixed azo dye- and Cr-contaminated soil. It was found that interaction between Cr and azo dye prevented the premature precipitation into the soil matrix and enhanced the removal rate of organic pollutants and heavy metals (Ricart et al., 2008). When EKR is applied to textile wastewater–contaminated soil, the removal of inorganic salts and metal ions conforms to the characteristic of electromigration and electroosmosis, but the Cu^{2+} anomaly migrates to the anode zone. It is implied that Cu^{2+} and organic groups recombine and migrate to the anode with the organic groups during the EKR process (Annamalai et al., 2014).

Soil and sediment physico-chemical characteristics near the electrodes will be greatly impacted on by electrolysis reactions at the early stages of the EKR. The electrolytic reactions are shown in Eqs. (1) and (2):

$$Anode: 2H_2O-4e^-\rightarrow O_2\uparrow + 4H^+; E_0 = -1.229V \quad (1)$$

$$Cathode: 2H_2O + 4e^-\rightarrow H_2\uparrow + 2OH^-; E_0 = -0.828V \quad (2)$$

where E_0 is the standard reduction potential.

At the anode, water loses electrons, generating H^+ and O_2, and the created H^+ ions move to the cathode electrolysis cell under the electric field, which can make the heavy metals in the soil dissolve into the pore water and improve the movement rate (often also the removal rate) of heavy metals, but excessive numbers of H^+ ions at the anode are easy to lead to soil acidification, corrosion of anode materials, and even a change in the direction of the electro-osmosis flows (Wang et al., 2021).

At the cathode, water is reduced leading to the production of hydrogen gas and hydroxide ions, generating OH^- and H_2 ions. The generated OH^- ions move to the anode under the action of the electric field. In the process of OH^- migration, heavy metal ions may precipitate before reaching the cathode (namely the focusing effect), which reduces the movement rate of heavy metals and hinders the removal of heavy metals in soil (Wu et al., 2021).

There are three situations that will lead to the relative increase of voltage near the electrode (namely the polarization effect) and affect the efficiency of EKR: (1) the concentration polarization caused by the concentration difference between the solution near the electrode and the bulk solution; (2) the resistance polarization caused by a layer of insoluble insulating salt or other insoluble impurities on the cathode surface inhibits the soil conductivity and decreases the current density; and (3) the activated polarization caused by the bubbles (composed of H_2 and O_2 or other gases) on the electrode surface. When they cover the respective electrode surface, the conductivity between the electrode and the electrolyte will be reduced. The polarization effect will hinder the migration of ions and affect the speed of electrodialysis (Lucas et al., 2019; Rojo et al., 2012).

In addition, soil heterogeneity and voltage gradient are key factors affecting the EKR. Soil mineral composition and buffering capacity affect the pollutant transportation rate. Saturated water content and low ionic strength of soil are the most favorable conditions for electroosmosis and pollutant migration. When the soil plasticity value exceeds 35, the soil will shrink excessively during the remediation process, leading to soil cracking and disturbing the pollutant removal mechanism (López-Vizcaíno et al. 2016a, b). The range of voltage gradient used in laboratory tests is 1–3 V/cm (Li et al., 2018; Zhu et al., 2009). The high current level can increase the total ion concentration and improve the ion electromigration efficiency in the electro-kinetic remediation process (Tang et al., 2020), but it will reduce the overall electroosmotic flow and release a lot of heat (Joule effect), resulting in energy consumption and relatively high costs (Xue et al., 2017).

2.2 Models

Numerical models can be useful tools to further understand and predict the processes that influence the efficiency of EKR and to precisely design, optimize, and

control EKR systems (Sprocati et al., 2019). When dealing with extremely complicated and challenging variables, modeling before starting an operation can significantly reduce the time and cost of such a process by allowing an accurate prediction of possible outcomes.

Cabrera-Guzmán et al. (1990), Acar et al. (1993), and Probstein and Hicks (1993) assimilated the traditional electrochemical, soil colloid dual-mode and mass transfer theories, and established a preliminary thermodynamic model to describe conduction phenomena under electrical and hydraulic potentials. In the presence of hydraulic, electrical, and chemical gradients, the one-dimensional total flux of species j per unit area of the soil medium is given by Acar and Alshawabkeh (1993) in Eq. (3):

$$J_j = -D_j^* \frac{\partial C_j}{\partial x} - C_j \left(u_j^* + k_e \right) \frac{\partial E}{\partial x} - C_j k_h \frac{\partial h}{\partial x} \qquad (3)$$

where J_j is the total flux of species j, D^* is the effective diffusion coefficient of species j, C_j is the concentration of species j, u^* is the effective ionic mobility, E is the electric potential difference, k_e is the electroosmotic coefficient of permeability, h is the hydraulic head, k_h is the hydraulic conductivity of the soil, and x is the linear distance.

The theoretical and experimental results showed that the electrical potential difference profile across the specimen is non-linear. The efficiency of removal of a specific species will decrease in time as its concentration with respect to other species in the pore fluid decreases (Acar & Alshawabkeh, 1993). Although the early electric remediation models can estimate the total mass flux of contaminants, and simulate the acid-base distribution in the system as well as analyze the relative contribution of electroosmosis and electromigration (Acar et al., 1993), these models are based on the assumption of homogeneous porous media, and most of them adopt indoor simulation such as kaolin. Therefore, there are still some limitations for the applications of electro-kinetic models to large-scale experiments.

Models of electro-kinetic soil remediation systems have been developed significantly in recent decades (Table 2). In 2002, an electromigration transport model for ion transport in unsaturated soil was developed by Mattson et al. (2002a). The numerical model was based on the groundwater flow and transport codes MODFLOW and MT3D, which have been modified to account for electrically induced ion transport.

Most past studies were concerned with determining the residual contaminant distribution in the soil and measuring the overall removal efficiency after the electro-kinetic treatment. Al-Hamdan and Reddy (2008) developed the computer model EKGEOCHEM (ELECTROKINETIC GEOCHEMICAL) to calculate the concentration of any chemical species during electro-kinetic remediation as a function of time and space. It is generally accepted that the most consistent theoretical model for macroscopic EKR processes consists of the combination of mass balance equations coupled with the electro-neutrality condition, where the main transport mechanisms are electro-migration for charged species and electro-osmosis for neutral (non-charged) species (Jacobs & Probstein, 1996; Rodríguez-Maroto & Vereda-Alonso, 2009).

Few studies have been conducted with models that simulate the transport of heavy metals by including the process of switching electrodes, because of the complexity involved with the changes in the initial conditions. Sun et al. (2019) established a piecewise model to simulate the transport of Cd under a superimposed electric field. This research indicated progressive soil acidification; the "focusing" region of Cd was compressed by the migration of the acid front. The removal efficiency can be optimized by modeling and switching electrodes.

The most advanced simulators typically include the coupling of the physical mass transfer processes with geochemical databases to simulate EKR in saturated porous media (Sprocati et al., 2019). Sprocati et al. (2019) propose a multi-dimensional modeling approach that allows for the integrated description of fluid flow, solute transport (including electromigration and electro-osmosis), coulombic interactions between transported species, and a wide range of kinetic and equilibrium reactions. The proposed modeling tool NP-Phreeqc-EK is a coupling between COMSOL Multiphysics, which is applied to solve fluid flow and solute transport challenges in saturated porous media based on the Nernst-Planck-Poisson formulation, and PhreeqcRM, which is used to solve geochemical reactions. López-Vizcaíno et al. (2017) proposes a conceptual and numerical model that includes geochemical speciation other than the phenomena that have been described by other studies. The results show that the buffering system of carbonates affects the temporal evolution and spatial distribution of pH. They emphasize that simulations using realistic geochemical systems are critical.

Table 2 Different models of electro-kinetic remediation

Model	Features	Mathematical equations	Parameters	Source
DIFFUSE	The model provides a first-order, mathematical framework to examine the flow patterns and chemicals generated in electro-osmosis. The advantage of this model and the application of the finite element method are that they provide a mean to estimate the distribution of chemical species throughout the medium. Assumption: a constant current and a hydraulic potential difference are applied initially across a water saturated, homogeneous specimen of clay. Furthermore, it will be considered that dilute, ideal electrolyte solution properties apply in the presence of an inert matrix. Numerical implementation: a computer program (DIFFUSE) has been written in FORTRAN to solve the differential equation using 10 elements.	$q_{tc} = q_{cc} + q_{ch} + q_{ce}$ The total mass transfer expressed by the Nernst-Planck equation: $q_{tc} = \left[-D_J \frac{\partial C_J}{\partial x} + V_x C_J - \frac{zF}{RT} D_J C_J \left(\frac{\partial \phi}{\partial x} \right) \right] n dA$ The solute flux due to chemical potential gradients is given by Fick's First Law: $q_{cc} = -D_x \left(\frac{\partial C_J}{\partial x} \right) n dA$ $D_x = V_x + D^*$ $D^* = \rho D_0$ The solute flux due to hydraulic gradients (the Darcy's law): $q_{ch} = -k_x \left(\frac{\partial h}{\partial x} \right) n C_J dA$ $q_{tc} = \left(k C_J - D^* \left(\frac{\partial C_J}{\partial x} \right) \right) n dA$ $k = -\frac{zF}{RT} D^* \left(\frac{\partial \phi}{\partial x} \right) - k_e \left(\frac{\partial \phi}{\partial x} \right) - k_x \left(\frac{\partial h}{\partial x} \right)$ $= -k_m - k_{EO} - k_h$ The mass balance for H ions across the element requires $\nabla q_{tc} = -R \left(\frac{\partial C}{\partial t} \right) n dA$ $R = 1 + \rho_d k_p / \vartheta$ The gradient operator V for one-dimensional conditions renders $\left(\frac{\partial q_{tc}}{\partial x} \right) = -R \left(\frac{\partial C}{\partial t} \right) n dA$	q_{tc}- the total mass transfer q_{cc}- material influx due to chemical gradients q_{ch}- material influx due to hydraulic gradients which can incorporate the electro-osmotic flow q_{ce}- material influx due to electrical gradients D_J- diffusion coefficient C_J- the mass of solute per unit volume of solution x- flow direction V_x- average seepage velocity z- charge on the ion F- Faraday's constant (96,485 Coulombs) R- ideal gas constant T- temperature (K) ϕ- electrical potential n- the porosity of the medium A- section area D_x- the longitudinal dispersion coefficient in a saturated porous media D^*- the molecular diffusion coefficient ρ- a parameter that depends upon the porosity and tortuosity of the medium and varies between 0.13 to 0.49 D_0- the molecular diffusion coefficient in standard state k_x- the hydraulic conductivity of the medium h- the hydraulic potential k- a constant with units [L/T] representing the velocity of the species in the pore fluid k_e - the effective electroosmotic permeability of the soil $\partial C/\partial t$- the rate of mass change A- the area R- the retardation coefficient, a term representing the adsorption and desorption of ionic species on clay surfaces and/or any interactions between the different species leading to precipitation, or other chemical reactions: ρ_d- the dry (bulk) density of the soil k_p- the partition coefficient ϑ - the volumetric water content	Acar et al. 1993
MODFLOW-MT3D	The first model to describe electrically induced ion transport through variable saturated soil. However, the model does not account for electro-migration transport of cations located in the double layer.	The equation of continuity describing the transport of a non-reactive species through a unit volume of porous medium is: $J_i = D_i^* \nabla C_i + \mu_i^* C_i \nabla \phi + v C_i$	$\partial C_i / \partial t$- the change in concentration of component i in the unit volume with respect to time (mol·m⁻³·s⁻¹) J_i- the molar flux of component i (mol·m⁻²·s⁻¹)	Mattson et al., 2002a, 2002b

Table 2 (continued)

Model	Features	Mathematical equations	Parameters	Source
	Assumption: the electric potential field is constant with respect to time, which is an assumption that is valid for highly buffered soil or when the electrode electrolysis reactions are neutralized. Advective water movement through the soil due to either electric or hydraulic potentials was negligible. Numerical implementation: the linking code between two public domain groundwater flow (MODFLOW) and transport (MT3D) numerical codes was modified to allow these codes to predict ion transport due to an electric potential gradient.	$D_i^* = D_i \theta \tau(\theta)$ $\mu_i^* = \mu_i \theta \tau(\theta)$ $\mu_i = \mu_i^0 10^{\left(-0.5085 z_i^2 \left(\frac{\sqrt{I}}{1+\sqrt{I}}\right) - 0.3I\right)}$ $I = 0.127 EC_w - 0.003$ $EC_w = \dfrac{EC_b}{\left[\dfrac{F(\lambda)(\omega)^{n+2}}{(\omega)_{sat}}\right]}$ $\omega = \theta - \theta_0$ The governing equation for water flow is: $\nabla \cdot (K_{ii} \nabla h) - W = S_s \frac{\partial h}{\partial t}$ The governing equation for current flow is: $\nabla \cdot (EC_{aii} \nabla \phi) - J_r = 0$	D_i^* - the effective molecular diffusion coefficient of ion i in a porous medium ($m^2 \cdot s^{-1}$) C_r the concentration of component i μ_i^* - ion i effective ionic mobility in a porous medium ($m^2 \cdot V^{-1} \cdot s^{-1}$) ϕ- the electrostatic potential (V) v- the linear pore water velocity including the effects of both electroosmotic and hydraulic flow ($m \cdot s^{-1}$) D_r the molecular diffusion coefficient in water ($m^2 \cdot s^{-1}$) θ- the volumetric moisture content τ- the tortuosity μ_i- the ionic mobility of ion i in water ($m^2 \cdot V^{-1} \cdot s^{-1}$) z- the valence of ion i I- the ionic strength ($mol \cdot kg^{-1}$) EC_w- the electrical conductivity of a free solution ($S \cdot m^{-1}$) EC_b - the effective electrical conductivity of liquid phase within a porous medium including the effects of tortuosity and cross-sectional area of the liquid phase $F(\lambda)$, n - fitting parameters ω- the effective moisture contents θ_0- the immobile water content along the soil solid surface at which there is no ion flow through the bulk water K_{ii}- the hydraulic conductivity in the principle directions of flow ($m \cdot s^{-1}$) h- the hydraulic head (m) W- the volumetric flux rate per volume (s^{-1}) representing sources and sinks S_s- the specific storage (m^{-1}) EC_{aii}- the apparent electrical conductivity of the soil in the principle directions ($S \cdot m^{-1}$) J_r- the applied current at an electrode	Al-Hamdan & Reddy, 2008
EKGEO-CHEM	Applicable to predict the transport and speciation of heavy metals (chromium, nickel and cadmium) in soil during electro-kinetic remediation as a function of time and space. It is capable of predicting the chemical speciation of the contaminants as well as the form that they would exist within the soils. Assumptions: (1) electrical potential in the soil is constant with time; (2) surface complexation is applicable in the highly concentrated clay suspensions; (3) the effect of	Transport processes: $J_j = -D_j^* \frac{\partial C_j}{\partial x} - C_j \left(u_j^* + K_e\right) \frac{\partial E}{\partial x} - C_j K_h \frac{\partial h}{\partial x}$ (1) $D_j^* = D_j \tau m$ (2) $u_j^* = \frac{D_j^* z_j F}{RT}$ (3)	J_j- the molar flux of component i D_j^*- effective diffusion coefficient of species j C_j- concentration of species j x- the solute transport direction u_j^*- effective ionic mobility of species j K_e- electroosmotic permeability E- permittivity of the medium	

Table 2 (continued)

Model	Features	Mathematical equations	Parameters	Source
	temperature is negligible; (4) dissolution of soil is negligible; and (5) the system is at an equilibrium, the adsorption of Na^+ and K^+ to the solid surface and their adsorption competition with the metals are ignored. Numerical implementation: The Crank-Nicholson implicit finite difference technique is used to solve the main transport equations. The Newton-Raphson iterative solution technique is used to solve the resulting non-linear set of mass balance equations to determine the concentrations of all chemical species existing in the system.	$K_e = \frac{\varepsilon_0 \varepsilon \xi}{\eta} n$ (4) 1-D time-dependent equation for the transport of solute based on the conservation of mass: $\frac{\partial n C_j}{\partial t} = -\frac{\partial J_j}{\partial x} + n R_j$ Chemical reactions: the exponential Boltzmann expression: $\{X_S^Z\} = \{X^Z\}\left(e^{-\varphi F/RT}\right)^Z$ The relation between the activity of an ion and its concentration is given by: $\alpha_j = \gamma_j C_j$ $\log \gamma_j = -0.5 z_j^2 \left(\frac{\sqrt{\mu}}{1+\sqrt{\mu}} - 0.2\mu\right)$ $\mu = 0.5 \sum\limits_{j=1}^{n}\left(C_j z_j^2\right)$	K_h- hydraulic conductivity h- the hydraulic head D_f- diffusion coefficient of species j in free solution at infinite dilution τ- tortuosity factor n- soil porosity z_j- charge of species j F- Faraday constant R- ideal gas constant T- absolute temperature ε_0- permittivity in vacuum (8.854×10^{-12}C/V m) ε- permittivity of the medium ξ- zeta potential of the solid surface η- viscosity of the pore water t- time E- electrical potential H- hydraulic head R_f- production rate of the aqueous species j per fluid volume due to chemical reactions z- charge of ion X $\{X_S^Z\}$- activity of ion X of charge z near the surface $\{X^Z\}$- corresponding activity of X in bulk solution outside the influence of the charged surface $e^{-\varphi F/RT}$- the Boltzmann factor (Coulombic correction) α_j- thermodynamic activity of aqueous species j γ_j- activity coefficient of aqueous species j C_j- concentration of aqueous species j μ- ionic strength of the aqueous solution	
M4EKR	Applicable in natural unsaturated soils; and an extended geochemical system with 34 species that are involved in 24 chemical equilibria resulting from the presence of the most common major ions in many natural groundwater. Assumption: Isothermal conditions (298.15 K over the entire domain) and the gas pressure (GP) remains constant and equal to atmospheric pressure. Numerical implementation: the M4EKR model was implemented in Comsol Multiphysics, which is a partial differential equation solver based on the application of the finite element method with Lagrange multipliers.	Water transport: $\frac{\partial m_w}{\partial t} + \nabla \cdot I_w = 0$ $F_w = F_W^h + F_w^{eo} = \rho_w \cdot \left(q_W^h + q_W^{eo}\right) = \rho_w \cdot q_W$ Hydraulic flux contributions (Darcy's law): $q_W^h = -k_e^h (\nabla P_L + g \cdot \rho_w \cdot \nabla z)$ $k_e^h = k_{sat}^h \cdot k_{rel}^h = k_{sat}^h \cdot S_r^3$ Electroosmotic flux (semi-empirical Helmholtz-Smoluchowski formulation):	m_w- the mass of water per unit total volume (kg·m^{-3}) t- time ∇- the divergence operator I_w- the mass flow of water (kg·m^{-2}·s^{-1}) F_w- the mass flow of water F_W^h - hydraulic flux F_w^{eo} - the electro-osmotic flux ρ_w - the water density q_W^h - the hydraulic flow velocity	López-Vizcaíno et al., 2017

Table 2 (continued)

Model	Features	Mathematical equations	Parameters	Source
		$q_W^{eo} = -k_e^{eo} \cdot \nabla E = -k_{sat}^{eo} \cdot S_r^3 \cdot \nabla E$	q_W^{eo} - the electro-osmotic velocity	
		Chemical species transport:	q_w - water flow velocity	
		$\frac{\partial M_m}{\partial t} + \nabla \cdot F_m = R_m$	k_e^h - the effective hydraulic permeability of the soil	
		$M_m = \phi \cdot S_r \cdot \rho_w \cdot C_m$	P_L - liquid pressure	
			g - gravity	
			z - the vertical coordinate	
		$F_m = F_m^h + F_m^{eo} + F_m^{em} + F_m^{dif}$	k_{sat}^h - the saturated permeability	
		$F_m^h = F_w^h \cdot C_m$	k_{rel}^h - the effective hydraulic permeability of the soil	
		$F_m^{eo} = F_w^{eo} \cdot C_m$	S_r - the degree of saturation of the soil	
		$F_m^{em} = \rho_w \cdot \sum_{i=1}^{N} \alpha_i^m \cdot C_i \cdot q_i^{em}$	k_e^{eo} - the effective electroosmotic permeability of the soil	
		$F_m^{dif} = -\rho_w \cdot \sum_{i=1}^{N} \alpha_i^m \cdot D_i \cdot \nabla C_i$	E - the electric potential	
		$q_i^{em} = -\mu_i^e \nabla E$	k_{sat}^{eo} - the saturated electro-osmotic permeability	
		$\mu_i^e = \phi \cdot S_r \cdot \tau \cdot \gamma_i \cdot \mu_i^0$	M_m - the total mass of component m per unit total volume $(\text{mol} \cdot \text{m}^{-3})$	
		$D_i^e = \phi \cdot S_r \cdot \tau \cdot \gamma_i \cdot D_i^0$	F_m - the total molar flux of component m $(\text{mol} \cdot \text{m}^{-2} \cdot \text{s}^{-1})$	
		$\mu_i^0 = \frac{D_i^0 \cdot F}{RT}$	R_m - the rate of production or consumption of component m $(\text{mol} \cdot \text{m}^{-3} \cdot \text{s}^{-1})$.	
		Transport of electric charge:	ϕ - the porosity	
		$\frac{\partial Q}{\partial t} = \nabla \cdot I = R_Q$	C_m - the total molar concentration of component m $(\text{mol} \cdot \text{kg}^{-1} \cdot \text{w}^{-1})$	
		$I = -\sigma_a \cdot \nabla E$		
		$\sigma_s = 0.023 \cdot \%_{clay} - 0.0209$	F_m^h - advective flow generated by the hydraulic gradient	
		$\sigma_w = \sum_{i=1}^{N} \left(\lambda_{0,i} \cdot \gamma_i \cdot C_i \right)$	F_m^{eo} - advective flow generated by the electrical gradient	
		$\nabla \cdot I = 0$		
		Mass balance in electrolyte wells:	F_m^{em} - electro-migratory flow	
		$\frac{\partial M_m}{\partial t} = M_m^{in} - M_m^{out} + M_m$	F_m^{dif} - diffusive-dispersive flow	
		Chemical speciation equations:	α_i^m - the molar contribution to the total concentration of component m of species i	
		$C_m - C_m^{cal} = 0$	C_i - the molar concentration of the species	

Table 2 (continued)

Model	Features	Mathematical equations	Parameters	Source
		$C_m^{cal} = \sum\limits_{i=1}^{N} \alpha_i^m C_i = \sum\limits_{i=1}^{N} \alpha_i^m \frac{\alpha_i}{\gamma_i}$ $\log(\alpha_i) = \log(K_i^{eq}) + \sum\limits_{m=1}^{M} \left(\alpha_i^m \cdot \log(\alpha_m)\right)$	q_i^{em} - the migration velocity D_i - effective diffusion/dispersion coefficient μ_i^e - values of the ionic mobility τ - the tortuosity of the medium γ_i - the coefficient of activity of species i μ_i^0 - its ionic mobility at infinite dilution in water D_i^e - the effective diffusion coefficient of each species D_i^0 - the binary diffusion coefficient in water z - the charge number of species F - Faraday constant R - ideal gas constant T - the temperature Q - the total electric charge (C·m^{-3}) I - the total current density (A·m^{-2}) R_Q - the rate of generation/consumption of the electric charge (C·m^{-3}·s^{-1}) σ_a - the apparent electrical conductivity σ_s - the conductivity of the solid phase $\%_{clay}$ - the weight percentage of the clay soil particles considered σ_w - the conductivity of the aqueous phase $\lambda_{0,i}$ - the ionic molar conductivity of species i M_m - the mass input rate (superscript in) or mass output rate (superscript out) in the well of component m (mol·s^{-1}) M_m^{in} - the mass input rate (superscript in) in the well of component m M_m^{out} - the mass output rate (superscript out) in the well of component m R_m - the rate of production or consumption of the component (mol·s^{-1}) C_m - the variables of the state of the equilibrium equations described above	

Table 2 (continued)

Model	Features	Mathematical equations	Parameters	Source
			C_m^{cal} - the molar concentrations of component m in the acolyte and catholyte α_i^m - the molar contribution of species i to component m. K_i^{eq} - the equilibrium constant of the formation reaction of i	
NP-Phreeqc-EK	Allows the integrated description of fluid flow, solute transport, Coulombic interactions between transported species, and a wide range of kinetic and equilibrium reactions. The distinguishing features of the proposed model are: (i) the solution of the Nernst–Planck–Poisson equations to accurately describe the Coulombic interactions coupling the displacement of charged species in porous media and to comply with the electro-neutrality condition; and (ii) the flexible integration with a geochemical database allowing the simulations of kinetic and equilibrium reactions occurring both in the pore solution and at the solid/liquid interface. Assumption: only water reduction at the cathode and oxidation at the anode. Numerical implementation: the proposed model for electro-kinetic transport in porous media, based on the Nernst–Planck–Poisson formulation, is implemented by coupling a flow and transport simulator with a geochemical code.	The transport of charged species: $\mu_i = \mu_i^0 + RT\ln(a_i) + z_i F\phi$ The Nernst–Planck equation: $J_i^{Tot} = \underbrace{-nD\nabla C_i}_{J_i^{Dif}}\underbrace{-nD_iC_i\nabla\ln(\gamma_i)}_{J_i^{act}}\underbrace{-nD_i\frac{z_iF}{RT}C_i\nabla\phi}_{J_i^{Mig}}+\underbrace{q^*C_i}_{J_i^{Adv}}$ $q^* = q + u_{eo} = \underbrace{\frac{K_h}{\mu}\nabla h}_{q}-\underbrace{K_{eo}\nabla\phi}_{u_{eo}}$ The governing multicomponent ionic transport equation is given by a material balance: $\frac{\partial(nC_i)}{\partial t} + \nabla J_i^{Tot} = r_i$ The Poisson's equation for electrostatics: $\nabla^2\phi = \frac{\rho_e}{\varepsilon}$ The electric current and the charge balance: $I = F\sum_{i=1}^{N} z_i J_i^{Tot}$	μ– the electrochemical potential μ_i^0– the electrochemical potential in standard conditions R– the ideal gas constant T– the temperature a_i– the activity of the ion in solution z_i– its valence F– the Faraday's constant ϕ– the electrostatic potential J_i– the molar flux of component i D_i^{aq}– the aqueous diffusion coefficient C_i– the concentration of species i γ_i– the coefficient of activity of species i J_i^{Tot}– the total flux of a species i n– the accessible porosity D_i– the pore diffusion/dispersion coefficient q^*C_i– the advective flux of species i q– the specific discharge resulting from piezometric head differences u_{eo}– the electroosmotic velocity K_h– the hydraulic conductivity μ– the dynamic viscosity ∇h– the piezometric head gradient K_{eo}– the electroosmotic permeability r– the reactive source/sink term ρ_e– electric charge density ε– the absolute permittivity of the medium I– electric current flux F– the Faraday constant	Sprocati et al., 2019
SE-EK Model	Simulate and optimize the process of Cd transport in soil under the superimposed electric field.	The total mass flux:	J_i – the total mass flux under an electric field in porous media of soil	Sun et al., 2019

Table 2 (continued)

Model	Features	Mathematical equations	Parameters	Source
	Assumptions: (1) the soil is isotropic and isothermal; (2) soil particles are non-conductive and their surface conductivity is negligible; (3) electrophoresis can be ignored; (4) the hydraulically driven advection flow is negligible, because of its lower order of magnitude compared to electroosmotic flow; (5) the pore geometry characteristics do not change over time; and (6) the precipitate of $Cd(OH)_2$ can be completely dissolved when the soil pH is sufficiently low. Numerical implementation: the numerical model was implemented by MATLAB 7.0 with a finite difference method.	$J_i = -D_i^*\nabla C_i - C_i(\mu_i^* + K_{eo}^e)\nabla\phi$ $\frac{\partial C_k}{\partial t_k} = -\frac{1}{\theta}\frac{J_k}{\partial x} + R_k$ $C_k^{initial} = C_{k-1}$ The partial differential equation that describes the transport of mass in porous media of soil under the constant electric field was evaluated as follows: $\theta\frac{\partial C_i}{\partial t} = D_i^*\frac{\partial^2 C_i}{\partial x^2} + (\mu_i^* + K_{eo})\frac{\partial C_i}{\partial x}\frac{\partial\psi}{\partial x} + \theta R_i$ (2) $R_{ad} = -\frac{\rho}{\theta}\frac{\partial S_i}{\partial t} = -\frac{\rho}{\theta}\frac{\partial S_i}{\partial t} = -\frac{\rho}{\theta}\frac{\partial c_c^i}{\partial t}$	D_i^* - the effective diffusion coefficient of the i-th species (m²·s⁻¹) C_i - the concentration of the i-th species in the aqueous phase (mol·m⁻³) μ_i^* - the effective ionic mobility of the i-th species (m²·V⁻¹·s⁻¹) K_{eo}^e - the effective electro-osmosis permeability coefficient in soil ϕ- the electric potential (V) C_k - the concentration of the Cd^{2+} in the aqueous phase θ - the volumetric moisture content J_k - the total mass flux of Cd^{2+} in porous media R_k- the production rate of the Cd^{2+} due to chemical reactions K_{eo}- the effective electro-osmosis permeability coefficient in soil (m²·V⁻¹·s⁻¹) R_i- the production rate of the i-th species due to chemical reactions R_{ad}- the production rate of the i-th species due to adsorption/desorption ρ - the bulk dry density of the soil S- the adsorbed concentration (mol·kg⁻¹)	Matteo et al. 2017
Local chemical equilibrium (LCE) model	This model is combined with the solution of the transient equations for the kinetics of those chemical reactions that have representative rates in the same order than the transport mechanisms. Assumption: the solid matrix is formed as a combination of a chemically inert part consisting mainly of silicate and aluminosilicate minerals such as quartz and feldspar, and another part consisting of carbonates such as calcite and magnetite, which is soluble in acid media. The rate of dissolution of calcite follows the general rate law. Numerical implementation: the numerical procedure presented in this work was achieved by coupling two specialized software packages, namely COMSOL Multiphysics and PHREEQC. COMSOL was used for the solution of the finite element integration of the transient Nernst-Planck-electro-neutrality system of algebraic and partial differential equations, while the	The rate of dissolution of calcite is assumed to follow the general rate law: $\frac{\partial m}{\partial t} = k A_0\left(\frac{m}{m_0}\right)^\alpha$ $k = k_f\left[1 - \left(\frac{IAP}{K_{sp}}\right)^\beta\right]$ The mass transport equation based on the Nernst-Planck equation: $p\frac{\partial C_i}{\partial t} = \nabla\left[\frac{p}{\tau}(D_i\nabla C_i - (U_i + k_{eo})C_i\nabla\phi)\right] + pG_i$ The Nernst-Townsend-Einstein relation was applied to relate diffusivity to the ionic mobility: $U^i = \frac{D z_i F}{RT}$ The electric potential ϕ is computed by solving the current conservation equation:	m- the amount of solid (mol) k - the specific rate constant A_0- the initial specific surface area (m²·kg⁻¹) α- changes in the specific surface area of the particles during dissolution and k (mol·m⁻²·s⁻¹) k_f a forward constant (mol·m⁻²·s⁻¹) IAP - the ion activity product K_{sp} - the solubility product constant β - a coefficient related to the stoichiometry of the reaction ($\beta = 2/3$ for calcite, assuming spherical particles). p- the porosity C_i- the concentration (mol·m⁻³) τ- the tortuosity D_i- the diffusion coefficient (m²·s⁻¹) U_i- the ionic mobility (m²·s⁻¹·V⁻¹) k_{eo} - the electroosmotic permeability (m²·s⁻¹·V⁻¹) ϕ - the electric potential (V)	

Table 2 (continued)

Model	Features	Mathematical equations	Parameters	Source
	algebraic system of chemical equilibrium equations, accounting for the formation of aqueous complexes, precipitation and dissolution reactions, were computed using the PHREEQC.	$\nabla J = 0$ $J = -\sigma \nabla \phi = -p\pi\sigma_w \nabla \phi$	G_T – a volumetric net source due to chemical reactions (mol·m⁻³·s⁻¹) z_T – the ionic charge F – the Faraday constant (C·mol⁻¹) R – the ideal gas constant (J·K⁻¹·mol⁻¹) T – the temperature (K) J – denotes the current density (A·m⁻²) described by Ohm's law σ – the electrical conductivity (S·m⁻¹) σ_w – the pore fluid conductivity	Matteo et al., 2017
SEKRET Model	Optimization of field-scale electro-kinetic processes, which include the possibility of estimating optimum design parameters and minimizing the treatment costs. Assumption: neglected advective flow because of its lower order of magnitude compared to electroosmotic flow due to the low hydraulic permeability of the investigated material; the porous medium is isotropic and that the degree of water saturation is constant at 100%; the pore geometry characteristics (e.g., porosity and tortuosity) were assumed to remain unchanged over time; electrophoresis was neglected, since colloid migration is mostly hindered by the immobile phase of the sediment. Numerical implementation: in the first step, diffusion, electro-migration and electro-osmosis are computed with COMSOL Multiphysics, which solves the non-linear system of partial differential equations (Nernst-Planck equations) with the finite element method. In the second step, chemical reactions are calculated using PhreeqcRM. The coupling time step is arbitrarily selected low enough to minimize the split operator errors for the specific model implementation and high enough to ensure acceptable computation times. The time interval of each transport step is automatically adjusted by COMSOL to achieve convergence	The transport of dissolved chemical species: $n\frac{\partial C_i}{\partial t} = -\nabla\left[-D_i\nabla C_i - (U_i^* + k_{eo})C_i\nabla\phi\right] + nR_i \quad (1)$ The energy cost was calculated with the following relationship: $C_E = \frac{1}{U}(V + \Delta V_{AN} + \Delta V_{CAT})IE_C t \quad (2)$ The cost for acid was calculated assuming stoichiometric buffering of OH⁻ at the cathode: $C_A = \frac{1}{U}\frac{1}{F}\frac{A_C}{M_A}t \quad (3)$ The cost for the electrodes was estimated as follows: $C_{EL} = \frac{1}{U}(A_m L_{AN} C_{AN} + L_{CAT} C_{CAT}) \quad (4)$	n – the porosity C_i – the concentration of the i-th species D_i – the effective diffusion coefficient of the i-th species U_i^* – the effective ion mobility k_{eo} – the coefficient of electro-osmotic permeability (m²·V⁻¹·s⁻¹) ϕ – the electric potential R_i – the net source or sink of C_i due to chemical reactions C_E – the energy cost U – the volume of sediment in between one electrode couple (m³) V – the sediment voltage at the anode side (V) ΔV_{AN} – the voltage drop at the anode well (V) ΔV_{CAT} – the voltage drop at the cathode well (V) I – the electric current (A) E_C – the cost for electrical energy (€ W⁻¹·h⁻¹) t – the time required to decontaminate the sediments up to the target removal level (h) C_A – the acid unit cost (€ m⁻³) F – the Faraday constant A_C – the acid unit cost M_A – the concentration of the acid solution (mol·m⁻³) C_{EL} – the cost for the electrodes A_m – the anode amortization percentage L_{AN} and L_{CAT} – the length of the anode and cathode, respectively (both assumed to be 1-m long) C_{AN} and C_{CAT} – the costs for the anode and cathode, respectively	

In many cases, laboratory experiments can be excessively time-consuming, and modeling could become a necessary tool to assess the main remediation parameters and predict achievable results. Despite electro-kinetic applications have shown promising results, quantitative understanding of such systems is still challenging due to the complex interplay between physical transport processes, electrostatic interactions, and geochemical reactions in multiple dimensions (Sprocati & Rolle, 2020). To find the optimum set of design parameters for cost minimization is also a development trend of current research.

3 Technical Approaches to Improve Electro-kinetic Remediation Performances

The efficiency of EKR depends mainly on the activation such as desorption and dissolution of contaminants as well as migration of pollutants. However, some pollutants such as Hg, Cd, and HOC are relatively insoluble, and it is difficult to achieve adequate activation and migration with a single EKR. In addition, the pH value, the polarization of electrodes, and pollutant accumulation also affects the efficiency of EKR (Altin & Degirmenci, 2005; Isosaari et al., 2007). When a single EKR is conducted, heavy metal removal rates usually range between 14 and 59%, and the removal rate of organic pollutants ranges even between 9 and 61% (Table 3). Moreover, there are significant differences in the removal efficiency of different pollutants even if the same EKR technology is applied. In general, a single EKR is suitably used to optimize the mechanistic parameters for target pollutants in given contaminated soil and sediment. In order to enhance the mobility and removal rate of pollutants, and reduce the side effects, many techniques including separation and reaction of pollutants, electrolyte pH adjustment, electrode optimization, and multi-technology combination have been developed to improve EKR performance (Fig. 2).

3.1 Separation and Reaction of Pollutants

Organic complexing agents can react with difficult-to-dissolve heavy metals to form soluble complexes, which will improve the migration efficiency of heavy metals. NaClO can also be used as an oxidant for a catholyte (Cang et al., 2007). The efficiency of metal extraction through electro-kinetics was the highest when both the anodic and the cathodic chambers were conditioned with the complexing agent ethylenediaminetetraacetic acid. The following removal yields were obtained: 81% for As, 69% for Cr, 40% for Cu, 33% for Pb, and 22% for Zn (Andreottola et al., 2010). Adding potassium permanganate oxidant to the catholyte increased the removal rate of Cr from 32 to 78%.

Furthermore, López-Vizcaíno et al. (2018) presents an EKR study of soils polluted with 2,4-dichlorophenoxyacetic acid (a common polar pesticide), enhanced with an anolyte pH conditioning strategy. By using 0.1 mol/L NaOH as the anolyte, the removal rate of fluorine reached 70%. Moreover, applying NaOH not only enhances the remediation of fluorine-contaminated soil, but also enhances the removal potential of other anionic pollutants such as arsenate and chromate (Zhou et al., 2015).

An oxidant can change the solubility and degradation rate of pollutants. For example, mercury exists in natural soil in the form of HgS, Hg, and HgO. All of them have very low solubility, which results in the challenge of EKR to address Hg-contaminated soil challenges. In 1996, Cox et al. (1996) demonstrated the potential of iodine/iodide lixiviant for maintaining proper thermodynamic conditions for effective electro-kinetic remediation of Hg-contaminated soils, and more than 90% of Hg existed in the form of HgI_4^{2-}. The ultimate removal rate of Hg in contaminated soil reached 99%.

Adding a co-solvent can effectively increase the solubility of certain organic matter in the soil and reduce the adsorption of hydrophobic organic pollutants so that more organic matter can be removed from the contaminated soil by electroosmosis. A series of bench-scale electro-kinetic experiments indicated that phenanthrene was migrating toward the cathode in proportion to the concentration of n-butylamine. The extent of migration was dependent on the n-butylamine concentration and the strength of electroosmotic flow (Maturi & Reddy, 2008).

Adding surfactants to the contaminated soil can reduce the activation energy on the soil particles, which will achieve the purpose of removing pollutants by promoting desorption of pollutants. The non-ionic surfactant Tween 80 (Polysorbate 80) and the anionic surfactant sodium dodecyl sulfate (SDS) were used to aid desorption of PAH from the soil, and the removal rate of PAH reached a maximum of almost 87% (Lima et al., 2012). Tween 80, polyoxyethylene ether, modified cyclodextrin,

Table 3 Pollutant removal via electro-kinetic remediation with different soil properties

Pollutants	Soil property			Removal rate	Sources
	Type	Moisture content (%)	pH		
Cr	Artificial	13.5	7.48	59.0%	Lu et al. 2009
Cr(III)	Natural	30	/	20.9%	Meng et al., 2018
Cr(VI)	Artificial	/	3.76	37.6%	Almeira et al., 2012
Pb	Artificial	50-54	4.93-5.20	22.3%	Kim et al., 2005
Pb	Artificial	37.55	5.7	52.9%	Li et al. 2005
Cd	Artificial	50-54	4.93-5.2	14.2%	Kim et al., 2005
α-HCH	Natural	/	6.28	60.9%	Ni et al., 2018
P and P-DDT	Natural	/	6.28	40.0%	Ni et al., 2018
Phenanthrene	Artificial	/	/	9.4%	Sun et al., 2017
Trichlorophenol	Artificial	/	/	14.3%	Sun et al., 2017

and N-butyl amine are often used as the surfactants to improve EKR performance (Sun et al., 2017). The requirements of selecting complexing agents are that (a) the ligands should have high solubility in solutions with a wide pH range; (b) formers are not easy to adsorb on the soil surface; and (c) formers should be non-toxic or have low toxicity with little potential risk to the environment.

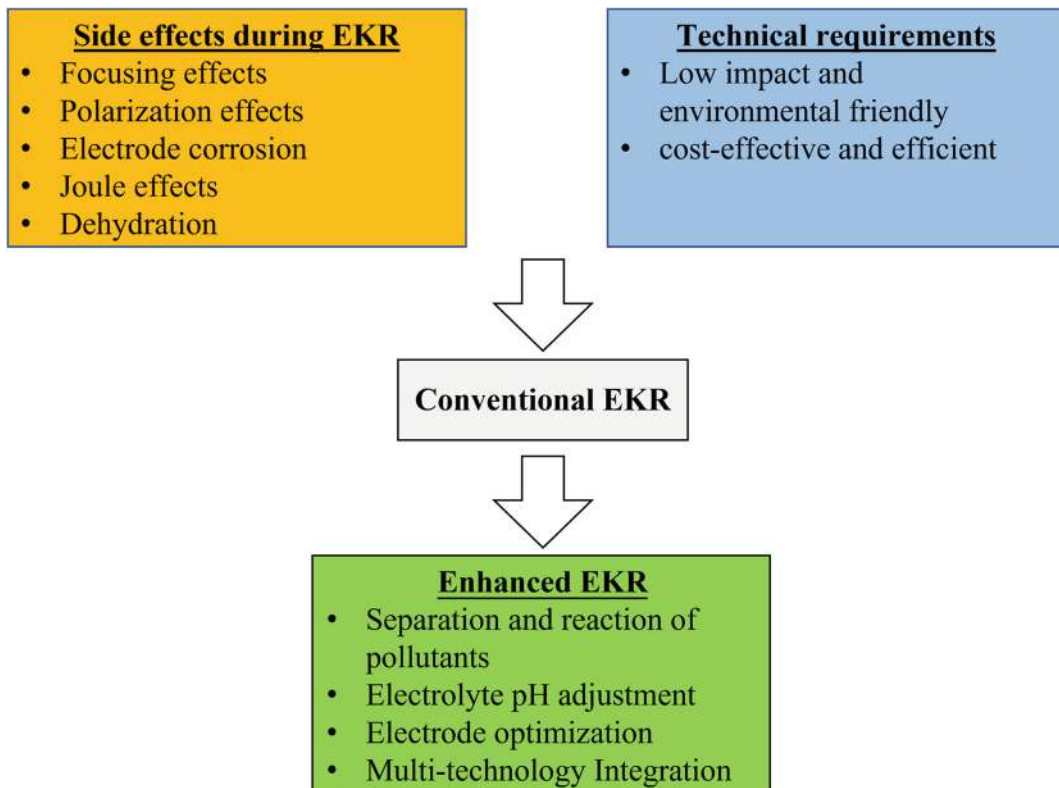Heating and stirring are considered as physical pre-treatment methods in this sub-chapter.

Fig. 2 Schematic diagram of the enhanced electro-kinetic remediation technology

Temperature mainly influences the ionic migration velocities, and can promote electromigration and electroosmosis as it increases. Increasing the soil and sediment temperature can accelerate the migration and diffusion of pollutants, which applies to ectopic EKR (Baraud et al., 1999). Elevating the soil temperature from 21 to 55°C reduced the time to extract potassium dichromate from kaolinite soils under saturated conditions. Conversely, increasing the soil temperature under dewatering conditions caused soil cracking, which reduces the overall process efficiency (Krause & Tarman, 1993).

Stirring is an alternative effective way to speed up the process of removing pollutants. It helps to enhance soil aeration and mixing, while increasing the bioavailability of pollutants. A stirred soil setup was applied when removing pollutants from heavily oil-contaminated soil with EKR, which led to removal efficiencies of up to 70% for total hydrocarbons and 65% for polyaromatic hydrocarbons (Pedersen et al., 2016). A combination of adding a surfactant and stirring was successfully used in the field of soil remediation to increase the removal efficiency of PAH by 79% (Lima et al., 2012).

3.2 Electrolyte pH Adjustment

Protons produced from the oxidation of organics at an anode result in anolyte acidification. Adding non-buffered saline catholyte effluent (e.g., from a previous cycle) to the anolyte leads to the mitigation of anolyte acidification (Davis et al., 2013). In addition, nitric acid can also induce the pH variations of the catholyte. For example, 0.06 M nitric acid has successfully been used to extract 98% of Cd from kaolin (Almeira et al., 2012). Adjusting the pH of contaminated soil can enhance the activity and the migration ability of pollutants during the electro-kinetic process, and thus increase the removal efficiency of the pollutants. Heavy metals are mainly present in the form of fractions of the following nature: exchangeable, carbonate-bound, Fe–Mn oxide bound, organic matter, and residual. Before EKR is performed, engineers have to add acids (acetic, lactic, humic, citric, ascorbic, and polyaspartic) to the soil to increase the concentration of dissolved heavy metals, and subsequently enhance the removal rate of heavy metals in soil by 15 to 59% (Fu et al., 2017; Zhou et al., 2004). Someone could also dissociate some organic matter into anions to accelerate the EKR process.

For example, by adjusting the soil pH to 9.3 with NaOH dissociated phenol and 2,4-DCP to obtain phenate anions, the mobility of phenol and 2,4-DCP can be increased by 2 and 5 times, respectively (Luo et al., 2005).

Inserting a cation exchange membrane and an auxiliary solution cell between the cathode and the soil has been proposed, which could make hydroxide ions generated by the electrolysis of water to be isolated within an auxiliary solution cell to prevent metal precipitation in the region near the cathode. This method was successfully used to treat Pb and Cd from artificially contaminated kaolin. Researchers observed an increase in the removal rates of Pb and Cd from 22% and 14% to 92% and 58%, respectively (Kim et al., 2005).

3.3 Electrode Optimization

This sub-chapter addressed the electrode optimization techniques' polarity exchange and approaching anodes. Methods to optimize electrode material, change the electrode structure and shape, and configure electrodes differently and pulse-power electrodes are also considered.

Polarity exchange could avoid the negative effect of OH^- on metal transportation, which makes the generation of H^+ ions from the oxidation of water neutralize the alkaline zone where the metal is precipitated, favoring its dissolution. The application of the polarity exchange method increased Mn removal from 14 to 72% in 7.6 days (Pazos et al., 2006). Applying electric fields always cause a dramatic change in soil microbial community structure. However, polarity exchange could effectively reduce negative effects on microbial communities (Kim et al., 2010).

The approaching anode electro-kinetic (AA-EK) method, which involves sequentially moving the anodic electrode approach to the fixed cathode, promotes the production of H^+, and increases the dissolution and removal of heavy metals and other pollutants, thus maintaining more mobile ions in the system and avoiding the "focus" effect (Shen et al., 2007; Tang et al., 2021). During the electro-kinetic process of approaching anodes, the energy utilization efficiency is increased, the migration and removal rates of Cd in soil can be increased by more than 1.5 times than the rates of conventional methods, and the remediation time is reduced by 40% (Shen et al., 2007).

Electrolysis reactions in the vicinity of electrodes may change the solubility and speciation of

contaminants (Zhou et al., 2004). Acidic conditions and electrolytic decay can corrode some anode materials (Davis et al., 2013); thus, the effect of electrode materials on the efficiency of electric repair should not be ignored. There are two types of optimizing electrode materials: changing the material of the electrode itself or coating active materials to the electrode surface layer. $Ti|IrO_2–Ta_2O_5$ was demonstrated as the best anode material in an EKR process, which showed the highest current density and corrosion-resistance (Méndez et al., 2012).

Changing the electrode structure can allow the pore water near the cathode to be drained fast and avoid the accumulation of hydroxyl, which greatly reduces the combination of heavy metals and hydroxyl to prevent the formation of deposits. An electro-kinetic geosynthetics electrode with flumes transformed from graphite electrodes can be used in experiments to remove Cd from paddy soil. The use of the EKG electrode avoided the corrosion of the anode and the formation of the precipitation of heavy metals near the cathode, which makes the separation rate of Cd in the paddy soil reach almost 42% (Tang et al., 2017).

The shape of the electrode also determines the strength and distribution of the electric field, which affects the migration rate of a pollutant. Using a ring electrode can more conveniently discharge pollutants compared with the use of a rectangular electrode structure. Moreover, under the same voltage gradient, the columnar electrode can produce a non-uniform electric field to greatly increase the electric field intensity in the center area compared to the plate electrode, which will improve the efficiency of the enrichment of organic pollutants at the cathode. After remediation, organic pollutant content in the center of the soil near the cathode can increase by between 98 and 124% (Luo et al., 2005; Mattson et al., 2002b; Musso, 2003).

Cylindrical electrodes can be installed in different configurations such as unidirectional, bidirectional, and radial-bidirectional as well as in form of radial pairs (Gill et al., 2014). Using an electrode matrix and making dynamic adjustments in a certain order can change the electric field distribution, which can also speed up the directional accumulation and separation of pollutants, promoting their degradation. Under a non-uniform electric field, a square electrode matrix of four electrode pairs was set, and the electric field distribution was adjusted every 3 h, which promoted the degradation of phenol. The phenol removal rate reached 58% after 10 days, and the high-frequency switching of the electric field distribution effectively prevented problems of uneven migration of pollutants in non-uniform electric fields (Luo et al., 2006).

Finally, the use of pulsed power can significantly reduce power consumption and improve the removal efficiency of heavy metals. Compared with traditional electric repair, using high frequencies (0.33–0.5 Hz) of the pulse power supply can effectively promote the desorption of ions near the anode, enhance their migration ability, and ultimately greatly improve the removal rate of heavy metals (Ryu et al., 2010).

3.4 Multi-technology Integration

3.4.1 Electro-kinetic Fenton

Advanced oxidation processes can promote the degradation of organic pollutants, thereby increasing their removal efficiency. Electro-kinetic Fenton is an electro-kinetic process that utilizes Fenton's reagent as a flushing solution (Fernández de Dios et al., 2014; Ng et al., 2014). The Fenton process produces hydroxyl radicals (·OH) by the reaction of hydrogen peroxide and ferrous ions ($Fe^{2+} + H_2O_2 \rightarrow Fe^{3+} + ·OH + OH^-$), and ·OH is a strong oxidant for most organic contaminants (Ni et al., 2018). The EK Fenton process can contribute to the transport of H_2O_2 through the soil. In the presence of iron or other transition metal minerals, this process decomposes H_2O_2 and generates ·OH and other oxidizing species such as $O_2^-·$ and $HO_2·$, which are capable of oxidizing contaminants (Paixão et al., 2020). Electro-kinetic Fenton was successfully applied to treat organic-contaminated soil, and the removal rates of α-HCH and P, P-DDT increased from 61% and 40% to 81% and 73 %, respectively (Ni et al., 2018).

3.4.2 Electro-kinetic Permeable Reaction Barrier

A permeable reaction barrier placed in a vertical flow direction can intercept contaminated water flows and remove pollutants through physical and chemical reactions. Such systems were originally used to prevent groundwater pollution (Mumford et al., 2015). Permeable reaction barriers composed of Pd/Fe were installed in pentachlorophenol-contaminated soil, and removed 49% of soil pentachlorophenol (Li et al., 2011). Research found that EKR technology combined with

permeable reaction barriers composed of zero-valent iron (Fe^0) can remove 80% of perchloroethylene from soil within 10 days, which was much higher than the removal rate of EKR technology alone (Kebria et al., 2016). The use of Fe^0/activated carbon as the permeable reaction barrier material in combination with EKR has also increased the removal rates of phenanthrene and trichlorophenol by 5 and 4.5 times, respectively (Sun et al., 2017).

3.4.3 Electro-kinetic Ultrasonic Technology

Ultrasonic technology has been used for wastewater treatment as an advanced oxidation process (Mahvi, 2009). When EKR is enhanced by ultrasonic technology, a larger current and stronger electroosmosis is generated, which greatly increases the removal rate of organic pollutants. When EKR is conducted for treating organic contaminated soil, using ultrasonic enhancement could increase the removal rate of organic pollutants by about 10% (Pham et al., 2009). Applying ultrasonic waves to the electro-repaired soil could also increase the enrichment of Cu^{2+} near the cathode by up to 43%, and thus improve the removal rate of heavy metals near the anode. However, the application of ultrasonic waves would cause variation of soil pH, making the acid zone more acidic and the cathodic zone more alkaline. Although the migration of heavy metal ions to the cathode could be promoted with the ultrasonic application, it is unable to solve the problem of cathode alkalization and precipitation (Blume & Neis, 2004).

3.4.4 Electro-kinetic Magnetic–Assisted Treatment

Electro-kinetic magnetic–assisted treatment is a type of technology that makes use of the effect of magnetic field on non-ferromagnetic fluid to change the properties of the pollutants in the traditional EKR process (Wu et al., 2013). The application of the magnetic field during electrolysis will increase the effective reaction area, and thus enhance the electrolysis reaction (Lin et al., 2017). Xie and Ma (2018) employed magnetic force–assisted EKR processes to remediate triclosan; the highest removal efficiency was 65% after 10 days of reclamation. Compared with the unenhanced EKR, the electro-kinetic magnetic technology promotes the electrolysis of water, enhances the electroosmosis, and promotes electro-kinetic magnetic migration of triclosan.

Electro-kinetic magnetic technology is low-cost and eco-friendly, enhancing the efficiency of pollutant removal.

3.4.5 Electro-kinetic-enhanced Bioremediation

Electro-kinetic-enhanced bioremediation technology uses a direct current electric field to drive the mass transfer between organic pollutants and degradation bacteria in the soil, enhancing the bioavailability of pollutants or use the current thermal effect and electrode reaction to provide appropriate temperature, pH, and redox conditions for the biotransformation process, and finally using microorganisms to degrade organic substances. In 2010, a bench-scale test demonstrated the potential to apply electro-kinetic-enhanced bioremediation for tetrachloroethene source remediation at a site in Skuldelev, Denmark (Mao et al., 2012).

3.4.6 Electro-kinetic Phytoremediation

Phytoremediation is relatively cheap and eco-friendly, but traditional phytoremediation approaches pose some limitations regarding their applications at large scale. So, there is a practical need to combine it with other technologies (Sarwar et al., 2017). In electro-kinetic phytoremediation, a redistribution of soil metals between electrode compartments and changes of plant uptake was compared with the absence of an electric field. The soil pH changes, normally decreasing in the anode compartment (Cang et al., 2011; O'Connor et al., 2003), which may lead to the activation of soil heavy metals in the anode region (Cang et al., 2011). Another study examined the effects of electro-kinetic amendments for phytoremediation of mixed contaminated soil, where typical silty clay soil was spiked with organic contaminants (naphthalene and phenanthrene) and heavy metals (lead, cadmium, and chromium). After 61 days of treatment, a significant reduction of heavy metals and organic contaminants in soil were detected (Chirakkara et al., 2015). For better improving the EKR performance, electro-kinetic phytoremediation could also be combined with other technologies such as electro-kinetic-ethylenediaminetetraacetic acid complexing-phytoremediation, and electro-kinetic-ethylenediamine-N,N'-disuccinic acid chelation-phytoremediation (Margarete & Thomas, 2001).

Table 4 Enhanced technologies and its performances

Enhanced method	Scale	Soil type	Pollutant	Electrode	Duration	Operating parameter	B (%)	P (%)	Source
Electrolyte pH adjustment	Soil column ø of 1.9 cm × 4 cm	Kaolin (60% water/soil ratio)	Cd	Titanium electrodes with iridium and ruthenium oxide coating	140 h	Injecting 0.06 M HNO₃ at a constant rate (0.6 mL/h) to induce the pH variations of the catholyte (0.01 M KNO₃).	39	98	Almeira et al., 2012
Electro-kinetic electrolyte enhancement	Soil column ø of 6.6 cm × 12 cm	Red soil (sieved through a 20-mm mesh sieve)	Cr (1009 mg/kg)	Square titanium alloy sheets of 3 cm × 3 cm	492 h	Adding oxidant: sodium hypochlorite (NaClO) as an oxidant in catholyte. Addition of the buffer solution to keep catholyte pH at 10.	7.4	72.0	Cang et al., 2007
Chemical pre-treatment and electrode optimization	Field plot experiments of 150 cm × 86 cm × 25 cm (width × length × height)	Sandy-loam (sand 50.1%, silt 42.6% and clay 7.3%)	Cd (0.83–1.04 mg/kg)	Novel electro-kinetic geosynthetics-based equipment	20 h	47.5 L of acid solution with a pH value of 2.31 that contained 0.03 mol/L FeCl₃ and 0.03 mol/L CaCl₂ was used to saturate cultivated soil layer.	25.93	41.98	Tang et al., 2017
Electro-kinetic electrolyte enhancement	Soil column ø of 3.2 cm × 10 cm	Kaolin	PAH	Graphite electrodes with a ø of 5.54 cm	23 days	Using pH control with 1% Tween 80 and 0.1M Na₂SO₄ as the processing fluid.	8.69	39.06	Alcántara et al., 2010
Electro-kinetic ion exchange membrane (EK-IEM)	10 cm × 15 cm × 10 cm (width × length × height)	Kaolinite (initial moisture content of about 52%)	Cd (1500 mg/kg) and Pb (5000 mg/kg)	Cathode electrode: titanium plate of 10 cm × 10 cm. Anode electrode: platinum plate of 10 cm × 10 cm	100 h	IEM-enhanced tests were undertaken using homogeneous IEMs (cation exchange membrane: Na-form; anion exchange membrane: Cl-form).	Cd (42.-64) and Pb (26.-74)	Cd (81.42) and Pb (54.46)	Kim et al., 2005
Electro-kinetic ion exchange membrane-auxiliary solution cell	10 cm ×15 cm × 10 cm (width × length × height)	Kaolinite (initial moisture content of about 52%)	Cd (1500 mg/kg) and Pb (5000 mg/kg)	Cathode electrode: carbon rode with a ø of 0.6 cm and a length of 10 cm. Anode electrode: stainless steel pipe of ø of 2 cm times length of 5 cm	100 h	Inserting the cation exchange Membranes and an auxiliary solution cell between the cathode and the soil.	Cd (22.-30) and Pb (14.-19)	Cd (91.60) and Pb (58.44)	Kim et al., 2005
Electrode optimization	20 cm × 15 cm × 15 cm (width × length ×	Sand (moisture content of 30%)	Cr	Rod-shaped graphite electrodes (length of 15 cm and Ø of 1 cm)	120 h	Multi-electrode system with polyaniline auxiliary electrodes.	40.06	60.11	Wang et al., 2021

Table 4 (continued)

Enhanced method	Scale	Soil type	Pollutant	Electrode	Duration	Operating parameter	B (%)	P (%)	Source
	height)					placed in the anode and cathode compartments, and polyaniline auxiliary electrodes (15 cm × 15 cm) were placed inside interlayers			
Electro-kinetic Fenton	30 cm × 10 cm ×15 cm (width × length × height)	Pesticide-contaminated soil, mainly of silt loam texture soil (moisture content of 35%)	Hexachloro-cyclohexane soprocide (HCH) and dichloro-diphenyl-trichloro-ethane (DDT)	Graphite electrodes (ø of 1.5 cm)	15 days	FeSO₄·7H₂O catalyst was added to the contaminated soil as a barrier of 5 mm × 100 mm × 120 mm (width × length × height) at a distance of 6 cm from the anode chamber; 10% H₂O₂ as the anolyte; 1% (mass fraction) β-cyclodextrin; and 0.2 M NaCl as flushing solution.	HCH (30.-5) and DDT (25.-9)	HCH (58.9) and DDT (47.6)	Ni et al., 2018
Electro-kinetic permeable reaction barrier and electro-kinetic electrolyte enhancement	4.5 cm × 4.5 cm × 6 cm (width × length × height)	Clay (passed through a 2 mm sieve; optimum moisture of 25%)	Tetrachlo-roethylene (PCE, 600 mg/kg)	Perforated graphite electrodes of 5 cm× 4 cm×0.5 cm (width × length × height)	10 days	Approximately 30 g of permeable reaction barrier material (zero-valent iron) was loaded into the permeable reaction barrier compartment. Triton X-100 was selected as the solubility enhancing agent.	4.8	58.7	Kebria et al., 2016
Electro-kinetic permeable reaction barrier and electrolyte pH adjustment	25 cm × 9 cm × 10 cm (width × length × height)	The surface soil (depth of 5–20 cm) was air-dried, grounded, and sieved through a 2-mm mesh	Phenanthrene	High-purity graphite electrodes (ø of 1 cm)	15 days	Biosurfactant-enhanced electro-kinetics coupled with a zero-valent iron/activated carbon permeable reactive barrier. The pH values of the catholyte were adjusted to 4 using NaOH (0.01 M) and	9.40	49.89	Sun et al., 2017

Table 4 (continued)

Enhanced method	Scale	Soil type	Pollutant	Electrode	Duration	Operating parameter	B (%)	P (%)	Source
Electro-kinetic ultrasonic	Soil column ø of 10 cm × 20 cm	Kaolin (moisture content of 1.03%)	Persistent organic pollutants: hexachlorobenzene, phenanthrene and fluoranthene	Titanium electrodes (ø of 1 cm × 10cm)	10 days	CH₃COOH (0.01 M) solutions. Ultrasound (24 kHz; 100 W).	53–71	70–83	Pham et al., 2009
Electro-kinetic magnetic–assisted treatment	20 cm × 10 cm × 10 cm (width × length × height)	Kaolin	Triclosan	Graphite electrodes	10 days	80 mT magnetic intensity was used to generate a magnetic field.	14.3	65.1	Xie et al. 2018
Electro-kinetic enhanced bioaugmentation	40 cm × 5 cm × 15 cm (width × length × height)	Gray and black clay (water content of 14 ±1%)	Chlorinated solvents (PCE and other chlorinated compounds)	Graphite plate electrodes	78 days	Delivering bioremediation additive into low-permeability soil and heterogeneous deposits.	—	The PCE concentrations decreased from several hundred to several dozens of mg/g at all ports	Mao et al., 2012
Electro-kinetic phytoremediation and electro-kinetic electrolyte enhancement	Laboratory-scale 24 cm × 24 cm × 25 cm (width × length × height)	—	Cu (2500 mg/kg), Cd (300–400 mg/kg) and As (230 mg/kg)	Cathodes of stainless steel and anodes composed of graphite chips	80–98 days	The catholyte was circulated between a reservoir and the two cathodes and was maintained at a pH of <5 by dosing with appropriate volumes of 8 M acetic acid to buffer the hydroxyl ions formed at the cathode.	—	/–	O'Connor et al., 2003
Pulsed electro-kinetic and electrolyte pH adjustment	4 cm × 4 cm × 20 cm (width × length × height)	Soil was sampled from a contaminated rice field (clay, 8.0%; silt, 50.3%; and sand, 41.7%)	Cd (12.7 mg/kg) and Zn (2322 mg/kg)	Plate-type graphite electrode (4 cm × 4 cm)	300 h	MgSO₄ (0.1 M) was employed to enhance the ionic strength of the soil bed.	Cd (12.-1) and Zn (15.-7)	Cd (30.7) and Zn (24.0)	Ryu et al., 2010.
			Fluorine		10 days		55.4	73.0	

Table 4 (continued)

Enhanced method	Scale	Soil type	Pollutant	Electrode	Duration	Operating parameter	$_B$ (%)	$_P$ (%)	Source
Electro-kinetic electrolyte enhancement	6 cm × 8 cm × 10 cm (width × length × height)	A cultivated surface soil (0–20 cm) was sampled near an aluminum smelting plant		Graphite sheet electrode of 6 cm × 8 cm ×1 cm (width × length × height)		Anolyte was circulated with NaOH solution, and catholyte was circulated with distilled water. Each electrolyte solution was refreshed every 24 h.			Zhu et al., 2009
Electro-kinetic phytoremediation and pulsed electro-kinetic process	20 cm × 20 cm × 18.5 cm (width × length × height)	Gray silty clay soil (clay, 42.0%; silt 42.0%; and sand 14.3%), and moisture content of approximately 15%	Pb (500 mg/kg), Cd (50 mg/kg) and Cr (200 mg/kg)	Graphite electrodes	61 days	Avena sativa (oat) and Helianthus annuus (sunflower) were selected as remediation plants. 25 V alternating current was applied to cells using graphite electrodes for 3 h per day.	Pb (24), Cd (17) and Cr (1-6-1-9)	Pb (25), Cd (17) and Cr (18–23)	Chirak-kara et al. 2015

Ø, diameter; $_B$ and $_P$, removal rates before and after enhanced technologies applied, respectively

3.5 Summary of Enhancement Technologies

The applicable conditions of current EKR improvement technologies are variable (Table 4). For pre-treatment technology, the addition of acid or oxidant is suitable for heavy metal separation, and adding an alkali, surfactant, or co-solvent is suitable for organic pollutant removal. It is difficult to increase soil temperature and stirring in practice. In general, electrode optimization is mainly used to repair heavy metal–contaminated soil and rarely to organic pollutants. Furthermore, multi-technology integration such as electro-kinetic ion exchange membrane, electro-kinetic electrolyte enhancement, and electro-kinetic phytoremediation are mostly used for heavy metal removal, and electro-kinetic Fenton, permeable reaction barrier, and ultrasonic or magnetic-assisted repair technologies are used for treating organic pollutants.

The removal rate of pollutants has been greatly improved after using enhancement technologies. Among them, the catholyte acidification method exhibited the largest increase in the removal rate of heavy metals by up to 67%. The greatest enhancement of organic pollutant removal is obtained by the electro-kinetic permeable reaction barrier, with an increased range between 40 and 50%. However, most of the current EKR enhancement technologies only promoted the migration and enrichment of pollutants, and the complete separation and removal of pollutants from the soil or sediment medium were not achieved. Therefore, the development of novel EKR enhancement technology should focus on pollutant separation via pore water drainage.

3.6 Critical Assessment of Laboratory Studies

Field plot experiments and bench scale tests in the laboratory show that the technology is applicable for diffusely dispersed pollutants in both the non-saturated and saturated media, and it is a promising in situ remediation technology. However, most experiments were conducted with sieved artificially contaminated soil or kaolin, and experimental pollutant contents are commonly higher than those in naturally contaminated soil (Table 4). Moreover, most bench-scale experiments were conducted in the laboratory within a soil column. The number of in situ cases and the volume of treated soil are relatively small. The size of the setup can lead to different conclusions. Hence, conclusions from small-scale tests should not be directly extrapolated to

full-scale applications (López-Vizcaíno et al., 2017). Laboratory test adopt artificial soil and pollutants, and the pore structure of contaminated soil as well as its content, form, and distribution of pollutants are quite different from actually polluted soil. Accordingly, the optimized parameters obtained in the laboratory cannot be directly used in the field test. The influence of uncertain factors such as influence of other contaminants, groundwater level, and soil types should be considered to bridge the gap between laboratory tests and field applications.

4 Technical Shortages and Solutions for Electro-kinetic Remediation

4.1 Variation in Soil or Sediment Physicochemical Properties

Due to EKR, storage of nutrients such as nitrogen, phosphorus, and potassium in the soil will be changed (Tang et al., 2018, 2020). After EKR of fluorine-contaminated field soil, the average soil available nitrogen content increased from anode to cathode, but the average available phosphorus and potassium content decreased, but the soil available potassium content gradually increased (Zhou et al., 2015). When the EKR was applied to Cd-contaminated soil, the average content of soil available nitrogen, phosphorus, and potassium increased by 0.44, 3.31, and 1.25 times in 60 h, while the content and morphology of organic carbon changed a little (Chen et al., 2006).

The literature review indicated that it is often easy to ignore the effects of EKR on the diversity of soil microorganisms and enzyme activities. During the practices of repairing pentachlorophenol-contaminated soil by EKR, the biomass of cultivable bacteria and fungi was decreased, and the respiration of soil microorganisms was weakened. Moreover, the use of carbon substrates significantly promoted the enrichment of pentachlorophenol around the anode (Lear et al., 2007). When EKR is conducted, a change in soil pH and an increase in toxicity of certain pollutants may also inhibit the reproduction of microorganisms and reduce microbial biomass and diversity (Kim et al., 2010). After EKR, the soil invertase and catalase activities increase, while soil urease and acid phosphatase activities decrease. Further correlation analysis shows that soil invertase and acid phosphatase activities are significantly related to soil

pH, electrical conductivity, and dissolved organic carbon content, which indicates that EKR can indirectly affect soil enzyme activities by changing soil physical and chemical properties (Cang et al., 2009).

In addition, electroosmosis also caused significant changes in soil and sediment moisture content, density, salinity, pH, redox potential, zeta potential, and cation exchange capacity, which led to the variation in soil and sediment microcosmic structure such as pore size distribution, and resulted in the accumulation of clay particles toward the cathode and anode (Korolev & Nesterov, 2019).

The effect of soil type and structure as well as the complexity of soil components on the efficiency of electro-kinetic treatment is less studied. The heterogeneity of soil itself leads to the migration and transformation of pollutants under the action of an electric field. Field studies are far more complex than indoor experiments. Therefore, it is important to strengthen the research in this aspect for the application of electro-kinetic remediation technology in the remediation of contaminated soil. The vast majority of contaminated sites are polluted by compounds. So, the development of electrically enhanced remediation technology for a variety of pollutants is one of the future development trends.

4.2 Difficulties in Field Application

Soil and sediment EKR technology mainly focused on laboratory research, and there are few applications for field practices. The effectiveness of in situ EKR depends largely on the chemical nature of the pollutants such as mobility, effectiveness, and the degree of homogenization of the sediment and soil particles (Reddy, 2010). Most of the EKR reactors are usually composed of electrodes (both anode and cathode), sample chamber, electrode chambers (both anode and cathode), and direct current power supply (Fig 1). The corresponding structure is relatively complex, which is not suitable for the field application. The following two shortages caused the limited in situ remediation practices of existing EKR technologies: the first one is the lack of an in situ EKR equipment for efficient separation and removal of pollutants. The second reason is the larger the scale of electric repair, the higher the energy consumption per unit volume of soil or sediment remediation, and the lower the removal rate of pollutants (López-Vizcaíno et al. 2016a, b; López-Vizcaíno et al., 2017).

Compared with soil, the moisture content of sediment is often high (Zhou et al., 2011), and pollutants are more easily to be migrated and subsequently be removed. So, EKR of contaminated sediment has a better application prospect (Fan et al., 2010). However, the existence of the overlying water and complicated below-water conditions hinders the application of EKR to in situ treatment of sediment, but EKR can be well used to reduce the sediment volume (Matteo et al., 2017; Tang et al., 2020) and remove harmful pollutants by the process of dewatering and electromigration. Furthermore, the behavior of the solid material is different in the field than in the laboratory, and scaling-up of the process is still challenging.

4.3 Novel Electro-kinetic Remediation Technology for Pollutant Separation and Drainage

Pore water is the main carrier of pollutants in soil and sediment (Booij et al., 2003). The rapid drainage of pore water can accelerate the transportation of pollutants, and separate pollutants from the soil or sediment matrix (Tang et al., 2020). At the same time, the enrichment of H^+ and OH^- near the electrode is weakened without adding any chemical reagents. This leads to the successfull alleviation of the polarization phenomenon.

In light of the technical shortage of traditional EKR, an integrated EKR technology for systematically considering pollution separation, drainage, and treatment was proposed (Fig. 3). The technical mechanisms and advantages of this novel technology are indicated below.

The novel EKG-based equipment exhibits obvious technical potential for field application. First, pollutants can be directly and completely isolated from the soil matrix through the efficient drainage of soil water. Second, rapid and excellent dewatering properties avoid the abundant accumulation of H^+ and OH^- near the electrodes and thus efficiently mitigate the anode acidic corrosion and cathode alkalization. Third, the equipment overcomes the shortcomings of having no facility for transporting the collected pore water to the cathode, installation difficulties, and having to maintain a large array of electrodes in the field for conducting EKG dewatering practices.

The EKG equipment is using an adsorption column to remove soluble pollutants such as NH_4^+ in the pore water. After completion of adsorption, the pore water is discharged into the electrolytic cell for electrolysis. The organic matter in the waste liquid is degraded by Fenton technology. The residual pollutants are subsequently filtered through the permeable reaction barrier and the
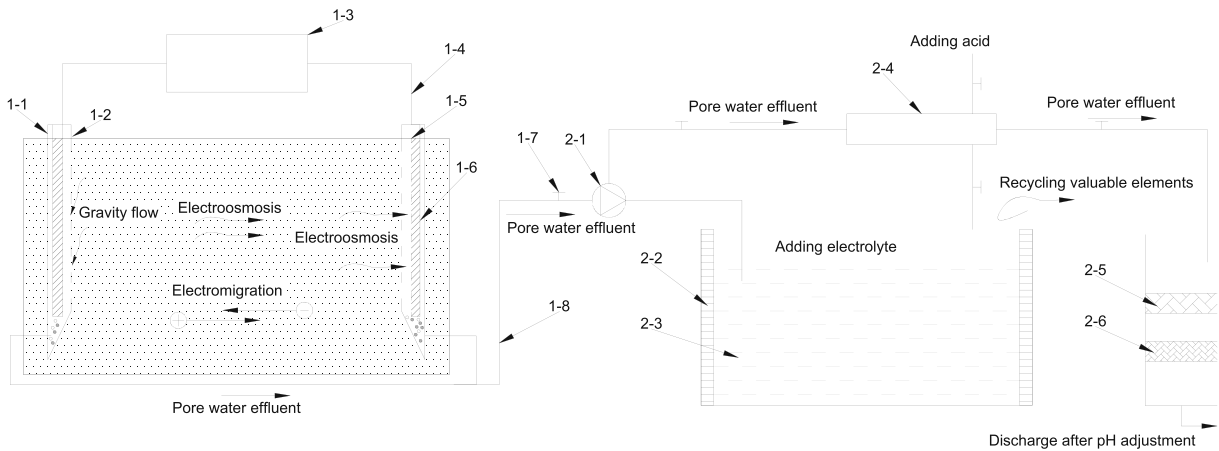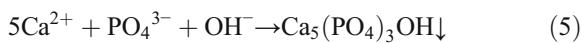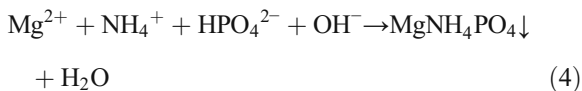
Fig. 3 Integrated electro-kinetic remediation technology based on pollutant separation, discharge and treatment. 1-1, pore water collector; 1-2, filter screen; 1-3, power supply; 1-4, waterproof wire; 1-5, cation exchange membrane; 1-6, electro-kinetic geosynthetics electrode; 1-7, control valve; 1-8, catheter; 2-1, pump; 2-2, electrode; 2-3, electrolyze; 2-4, humic acid resin adsorption column; 2-5, permeable reactive barrier; 2-6, chitosan (linear polysaccharide) flocculent

chitosan flocculent. Finally, the pH is adjusted before pore water discharge. Moreover, the valuable elements including nutrients can be recycled from the effluent during these processes.

Theoretically, phosphate will be enriched in the anode electrolyte, and the ammonium ion will be in the cathode. By adding magnesium oxide or lime to the anode electrolyte, neutralizing the pH of the anode electrolyte and mixing the cathode electrolyte, nitrogen, and phosphorus can be recovered in the form of magnesium ammonium phosphate (struvite) or hydroxyapatite through precipitation reaction as shown in Eqs. (4) and (5) according to the literature (Dai et al., 2017; Li et al., 2019).

$$Mg^{2+} + NH_4^+ + HPO_4^{2-} + OH^- \rightarrow MgNH_4PO_4\downarrow$$
$$+ H_2O \tag{4}$$

$$5Ca^{2+} + PO_4^{3-} + OH^- \rightarrow Ca_5(PO_4)_3OH\downarrow \tag{5}$$

5 Conclusions and Further Research Needs

Electroosmosis and electromigration dominates most of the pollutant removal via EKR. The current EKR models mainly focus on the process of ion transfer. As the main carrier of pollutants in soil and sediment medium, pore water migration and distribution should be studied to describe and reveal the mechanisms of EKR.

Electrolyte pH adjustment, electrode optimization, and multi-technology combination are mainly used to improve EKR performance. Commonly co-existing pollutants in soil and sediment behave differently in the electric field. Low soluble heavy metals are prone to be precipitated in the alkaline cathode zone, and organic pollutants are easy to adsorb to soil and sediment particles. These processes may hinder EKR performance.

The key to improve the efficiency of EKR is transferring pollutants from the solid to the liquid phase. To date, most EKR enhancement technologies only promote the migration and enrichment of pollutants near the electrode zone, but do not actually achieve the separation and removal of pollutants. Therefore, it is necessary to develop a novel EKR technology based on pore water drainage and associated pollutant separation.

The majority of research studies were conducted in the laboratory and focused on the EKR performance and mechanisms. It follows that limited studies address the practical issues due to shortage of in situ EKR equipment. Developing the mechanism model both considering the pore water and pollutant migration, distribution and removal is also recommended to reveal the actual EKR processes and optimize the technology parameters to guide the field applications.

Code Availability Not applicable. No custom code required.

Author Contribution All authors read and approved the final manuscript.

Funding Open access funding provided by Lund University.

Data Availability The authors confirm that the data supporting the findings of this study are available within the article.

Declarations

Conflict of Interest The authors declare that they have no conflict of interest.

Ethics Approval Not applicable. No animal or human participants.

Consent to Participate Not applicable. No animal or client participants.

Consent for Publication Not applicable. No individual person's data in any form.

References

Acar, Y. B., & Alshawabkeh, A. N. (1993). Principles of electrokinetic remediation. *Environmental Science & Technology, 27*(13), 2638–2647.

Acar, Y. B., Li, H., & Gale, R. J. (1992). Phenol removal from kaolinite by electrokinetics. *Journal of Geotechnical Engineering, 118*(11), 1837–1852.

Acar, Y. B., Alshawabkeh, A. N., & Gale, R. J. (1993). Fundamentals of extracting species from soils by electrokinetics. *Waste Management, 13*(2), 141–151.

Alcántara, M. T., Gómez, J., Pazos, M., & Sanromán, M. A. (2010). Electrokinetic remediation of PAH mixtures from kaolin. *Journal of Hazardous Materials, 179*(1-3), 1156–1160.

Al-Hamdan, A. Z., & Reddy, K. R. (2008). Transient behaviour of heavy metals in soils during electrokinetic remediation. *Chemosphere, 71*(5), 860–871.

Almeira, J., Peng, C. S., & Abou-Shady, A. (2012). Simultaneous removal of cadmium from kaolin and catholyte during soil electrokinetic remediation. *Desalination, 300*, 1–11.

Altin, A., & Degirmenci, M. (2005). Lead (II) removal from natural soils by enhanced electrokinetic remediation. *the. Science of the Total Environment, 337*(1–3), 1–10.

Andreottola, G., Bonomo, L., Gioannis, G. D., Ferrarese, E., Muntoni, A., Polettini, A., Pomi, R., & Saponaro, S. (2010). Lab-scale feasibility tests for sediment treatment using different physico-chemical techniques. *Journal of Soils and Sediments, 10*(1), 142–150.

Annamalai, S., Santhanam, M., Sundaram, M., & Curras, M. P. (2014). Electrokinetic remediation of inorganic and organic pollutants in textile effluent contaminated agricultural soil. *Chemosphere, 117*(1), 673–678.

Baraud, F., Tellier, S., & Astruc, M. (1999). Temperature effect on ionic transport during soil electrokinetic treatment at constant pH. *Journal of Hazardous Materials, 64*(3), 263–281.

Blume, T., & Neis, U. (2004). Improved wastewater disinfection by ultrasonic pre-treatment. *Ultrasonics Sonochemistry, 11*(5), 333–336.

Booij, K., Hoedemaker, J. R., & Bakker, J. F. (2003). Dissolved PCBs, PAHs, and HCB in pore waters and overlying waters of contaminated harbor sediments. *Environmental Science & Technology, 37*(18), 4213–4220.

Bruell, C. J., Segall, B. A., & Walsh, M. T. (1992). Electroosmotic removal of gasoline hydrocarbons and TCE from clay. *Journal of Environmental Engineering, 118*(1), 68–83.

Cabrera-Guzmán, D., Swartzbaugh, J. T., & Weisman, A. W. (1990). The use of electrokinetics for hazardous waste site remediation. *Journal of the Air & Waste Management Association, 40*(12), 1670–1676.

Cameselle, C., & Reddy, K. R. (2013). Effects of periodic electric potential and electrolyte recirculation on electrochemical remediation of contaminant mixtures in clayey soils. *Water Air Soil Pollut., 224*, 1636.

Cang, L., Zhou, D. M., Alshawabkeh, A. N., & Chen, H. F. (2007). Effects of sodium hypochlorite and high pH buffer solution in electrokinetic soil treatment on soil chromium removal and the functional diversity of soil microbial community. *Journal of Hazardous Materials, 142*(1–2), 111–117.

Cang, L., Zhou, D. M., Wang, Q. Y., & Wu, D. Y. (2009). Effects of electrokinetic treatment of a heavy metal contaminated soil on soil enzyme activities. *Journal of Hazardous Materials, 172*(2–3), 1602–1607.

Cang, L., Wang, Q., Zhou, D., & Xu, H. (2011). Effects of electrokinetic-assisted phytoremediation of a multiple-metal contaminated soil on soil metal bioavailability and uptake by Indian mustard. *Separation & Purification Technology, 79*, 246–253.

Casagrande, L. (1948). Electroosmosis in soils. *Geotechnique, 1*, 159–177.

Chen, X., Shen, Z., Lei, Y., Zhang, S., Ju, B., & Wang, W. (2006). Effects of electrokinetics on bioavailability of soil nutrients. *Soil Science, 171*(8), 638–647.

Chirakkara, R. A., Reddy, K. R., & Cameselle, C. (2015). Electrokinetic amendment in phytoremediation of mixed contaminated soil. *Electrochimica Acta, 181*, 179–191.

Chung, H. I., & Kamon, M. (2005). Ultrasonically enhanced electrokinetic remediation for removal of Pb and phenanthrene in contaminated soils. *Engineering Geology, 77*(3–4), 233–242.

Cox, C. D., Shoesmith, M. A., & Ghosh, M. M. (1996). Electrokinetic remediation of mercury-contaminated soils using iodine/iodide lixiviant. *Environmental Science & Technology, 30*(6), 1933–1938.

Dai, H., Lu, X., Peng, Y., & Zhsssu, H. (2017). Effects of supersaturation control strategies on hydroxyapatite (HAP) crystallization for phosphorus recovery from wastewater. *Environmental Science and Pollution Research, 24*, 5791–5799.

Davis, R. J., Kim, Y., & Logan, B. E. (2013). Increasing desalination by mitigating anolyte pH imbalance using catholyte effluent addition in a multi-anode bench scale microbial desalination cell. *ACS Sustainable Chemistry & Engineering, 1*(9), 1200–1206.

Fan, J. T., Miller, D. R., Zhang, L. W., & Sun, J. H. (2010). Effects of bark beetle pheromones on the attraction of *Monochamus alternatus* to pine volatiles. *Insect Science, 17*(6), 553–556.

Fernández de Dios, M. Á., Iglesias, O., Pazos, M., & Sanromán, M. Á. (2014). Application of electro-Fenton technology to remediation of polluted effluents by self-sustaining process. *The Scientific World Journal*, 801870. https://doi.org/10.1155/2014/801870.

Ferro, S., Rosestolato, D., & Bagatin, R. (2014). Electrokinetic remediation of soils polluted by heavy metals (mercury in particular). *The Chemical Engineering Journal, 264*, 16–23.

Forstner, U. (2004). Sediment dynamics and pollutant mobility in rivers: an interdisciplinary approach. *Lakes & Reservoirs Research & Management, 9*(1), 25–40.

Fu, R., Wen, D., Xia, X., Zhang, W., & Gu, Y. (2017). Electrokinetic remediation of chromium (Cr)-contaminated soil with citric acid (CA) and polyaspartic acid (PASP) as electrolytes. *Chemical Engineering Journal, 316*, 601–608.

Gill, R. T., Harbottle, M. J., Smith, J. W. N., & Thornton, S. F. (2014). Electrokinetic-enhanced bioremediation of organic contaminants: a review of processes and environmental applications. *Chemosphere, 107*, 31–42.

Isosaari, P., Piskonen, R., Ojala, P., Voipio, S., Eilola, K., Lehmus, E., & Itävaara, M. (2007). Integration of electrokinetics and chemical oxidation for the remediation of creosote-contaminated clay. *Journal of Hazardous Materials, 144*(1–2), 538–548.

Jacobs, R. A., & Probstein, R. F. (1996). Two-dimensional modelling of electroremediation. *AIChE Journal, 42*(6), 1685–1696.

Kebria, D. Y., Taghizadeh, M., Camacho, J. V., & Latifi, N. (2016). Remediation of PCE contaminated clay soil by coupling electrokinetics with zero-valent iron permeable reactive barrier. *Environmental Earth Sciences, 75*(8), 699.

Kim, W. S., Kim, S. O., & Kim, K. W. (2005). Enhanced electrokinetic extraction of heavy metals from soils assisted by ion exchange membranes. *Journal of Hazardous Materials, 118* (1-3), 93–102.

Kim, S. H., Han, H. Y., Lee, Y. J., Kim, C. W., & Yang, J. W. (2010). Effect of electrokinetic remediation on indigenous microbial activity and community within diesel contaminated soil. *the. Science of the Total Environment, 408*(16), 3162–3167.

Kim, L. Y., Choi, J. H., & Lee, Y. J. (2012). A Study on salt removal in controlled cultivation soil using electrokinetic technology. *Korean Journal of Soil Science & Fertilizer, 45* (6), 1230–1236.

Korolev, V. A., & Nesterov, D. S. (2019). Influence of electro-osmosis on physicochemical parameters and microstructure of clay soils. *Journal of Environmental Science & Health, Part A, 54*(6), 1–12.

Krause, T. R., & Tarman, B. (1993). Preliminary results from the investigation of thermal effects in electrokinetics soil remediation. *Farmakologiia i toksikologiia, 31*(1), 32–34.

Lear, G., Harbottle, M. J., Sills, G., Knowles, C. J., Semple, K. T., & Thompson, I. P. (2007). Impact of electrokinetic remediation on microbial communities within PCP contaminated soil. *Environmental Pollution, 146*(1), 139–146.

Lee, Y. J., Choi, J. H., Lee, H. G., Ha, T. H., & Bae, J. H. (2011). Pilot-scale study on in situ electrokinetic removal of nitrate from greenhouse soil. *Separation and Purification Technology, 79*(2), 254–263.

Li, A., Cheung, K. A., & Reddy, K. R. (2000). Cosolvent-enhanced electrokinetic remediation of soils contaminated with phenanthrene. *Journal of Environmental Engineering, 126*(6), 527–533.

Li, Z., Yuan, S., Wan, J., Long, H., & Tong, M. (2011). A combination of electrokinetics and Pd/Fe PRB for the remediation of pentachlorophenol-contaminated soil. *Journal of Contaminant Hydrology, 124*(1–4), 99–107.

Li, H., Muhammad, F., Yan, Y., Zhang, M., Jiao, B., Yu, L., & Li, D. (2018). Electrokinetic remediation of heavy metals from municipal solid waste incineration fly ash pretreated by nitric acid. *Royal Society Open Science, 5*(8), 180372.

Li, B., Huang, H., Boiarkina, I., Yu, W., Huang, Y., Wang, G., & Young, B. (2019). Phosphorus recovery through struvite crystallisation: recent developments in the understanding of operational factors. *Journal of Environmental Management, 248*, 109254.

Lima, A. T., Ottosen, L. M., Heister, K., & Loch, J. P. G. (2012). Assessing PAH removal from clayey soil by means of electro-osmosis and electrodialysis. *The Science of The Total Environment, 435–436* 1–6.

Lin, M. Y., Hourng, L. W., & Wu, C. H. (2017). The effectiveness of a magnetic field in increasing hydrogen production by water electrolysis. *Energy Sources, 39*(2), 140–147.

Lindgren, E. R., Mattson, E. D., Kozak, M. W. (1994). Electrokinetic remediation of unsaturated soils. *Emerging Technologies in Hazardous Waste Management IV*, chapter 3 (pp. 33–50). American Chemical Society Symposium Series, Vol. 554, Washington, DC: American Chemical Society.

López-Vizcaíno, R., Navarro, V., Alonso, J., Yustres, A., Cañizares, P., Rodrigo, M., & Sáez, C. (2016a). Geotechnical behaviour of low-permeability soils in surfactant-enhanced electrokinetic remediation. *Environmental Science and Health, 51*(1), 44–51.

López-Vizcaíno, R., Navarro, V., León, M. J., Risco, C., Rodrigo, M. A., Sáez, C., & Cañizares, P. (2016b). Scale-up on electrokinetic remediation: engineering and technological parameters. *Journal of Hazardous Materials, 315*, 135–143.

López-Vizcaíno, R., Risco, C., Isidro, J., Rodrigo, S., Saez, C., Cañizares, P., Navarro, V., & Rodrigo, M. A. (2017). Scale-up of the electrokinetic fence technology for the removal of pesticides. Part II: Does size matter for removal of herbicides. *Chemosphere, 166*, 549–555.

López-Vizcaíno, R., Yustres, A., Asensio, L., Saez, C., Cañizares, P., Rodrigo, M. A., & Navarro, V. (2018). Enhanced

electrokinetic remediation of polluted soils by anolyte pH conditioning. *Chemosphere, 199*, 477–485.

Lucas, M., Vahid, A., & Jay, M. (2019). Electro-osmosis treatment techniques and their effect on dewatering of soils, sediments, and sludge: a review. *Soils and Foundations, 59*(2), 407–418.

Luo, Q., Zhang, X., Wang, H., & Qian, Y. (2005). Mobilization of phenol and dichlorophenol in unsaturated soils by non-uniform electrokinetics. *Chemosphere, 59*(9), 1289–1298.

Luo, Q., Wang, H., Zhang, X., Fan, X., & Qian, Y. (2006). In situ bio electrokinetic remediation of phenol-contaminated soil by use of an electrode matrix and a rotational operation mode. *Chemosphere, 64*(3), 415–422.

Mahvi, A. H. (2009). Application of ultrasonic technology for water and wastewater treatment. *Iranian Journal of Public Health, 38*(2), 1–17.

Manokararajah, K., & Ranjan, R. S. (2005). Electrokinetic denitrification of nitrates in a nitrate contaminated silty loam soil. *Applied Engineering in Agriculture, 21*(3), 541–549.

Mao, T., & Pan, T. (2015). A multiphysics model for evaluating electrokinetic remediation of nuclear waste-contaminated soils. *Water Air Soil Pollut, 226*, 77.

Mao, X., Wang, J., Ciblak, A., Cox, E. E., Riis, C., Terkelsen, M., Gent, D. B., & Alshawabkeh, A. N. (2012). Electrokinetic-enhanced bioaugmentation for remediation of chlorinated solvents contaminated clay. *Journal of Hazardous Materials, 213–214*, 311–317.

Margarete, B. W., & Thomas, E. (2001). Environmental fate and microbial degradation of aminopolycarboxylic acids. *FEMS Microbiology Reviews, 25*(1), 69–106.

Matteo, M., Alessio, C., & Renato, I. (2017). Model-based optimization of field-scale electrokinetic treatment of dredged sediments. *Chemical Engineering Journal, 328*, 87–97.

Mattson, E. D., Bowman, R. S., & Lindgren, E. R. (2002a). Electrokinetic ion transport through unsaturated soil: 1. Theory, model development, and testing. *Journal of Contaminant Hydrology, 54*(1–2), 99–120.

Mattson, E. D., Bowman, R. S., & Lindgren, E. R. (2002b). Electrokinetic ion transport through unsaturated soil: 2. Application to a heterogeneous field site. *Journal of Contaminant Hydrology, 54*(1–2), 121–140.

Maturi, K., & Reddy, K. R. (2008). Cosolvent-enhanced desorption and transport of heavy metals and organic contaminants in soils during electrokinetic remediation. *Water, Air & Soil Pollution, 189*(1–4), 199–211.

Méndez, E., Pérez, M., Romero, O., Beltrán, E. D., Castro, S., Corona, J. L., Corona, A., Cuevas, M. C., & Bustos, E. (2012). Effects of electrode material on the efficiency of hydrocarbon removal by an electrokinetic remediation process. *Electrochimica Acta, 86*, 148–156.

Meng, F., Nie, L., Xue, H., & Zhang, D. (2018). Potassium permanganate oxidation-electrokinetic advanced remediation for soils contaminated with trivalent chromium. *Journal of Agro-Environment Science, 37*(6), 1125–1131 (in Mandarin).

Micic, S., Shang, J. Q., Lo, K. Y., Lee, Y. N., & Lee, S. W. (2001). Electrokinetic strengthening of a marine sediment using intermittent current. *Canadian Geotechnical Journal, 38*(2), 287–302.

Mumford, K. A., Powell, S. M., Rayner, J. L., Hince, G., & Stevens, G. W. (2015). Evaluation of a permeable reactive barrier to capture and degrade hydrocarbon contaminants. *Environmental Science & Pollution Research, 22*(16), 12298–12308.

Musso, G. (2003). Transport phenomena in electrokinetic soil remediation. *Mathematical & Computer Modelling, 37*(5–6), 589–594.

Ng, Y. S., Sen Gupta, B., & Hashim, M. A. (2014). Stability and performance enhancements of electrokinetic-Fenton soil remediation. *Reviews in Environmental Science and Bio/Technology, 13*, 251–263.

Ni, M., Tian, S., Huang, Q., & Yang, Y. (2018). Electrokinetic-Fenton remediation of organochlorine pesticides from historically polluted soil. *Environmental Science & Pollution Research, 25*(12), 12159–12168.

O'Connor, C. S., Lepp, N. W., Edwards, R., & Sunderland, G. (2003). The combined use of electrokinetic remediation and phytoremediation to decontaminate metal-polluted soils: a laboratory-scale feasibility study. *Environmental Monitoring & Assessment, 84*, 141–158.

Paixão, I. C., López-Vizcaíno, R., Solano, A. M. S., Martinez-Huitle, C. A., Navarro, V., Rodrigo, M. A., & Dos Santos, E. (2020). Electrokinetic-Fenton for the remediation low hydraulic conductivity soil contaminated with petroleum. *Chemosphere., 248*, 126029.

Pazos, M., Sanroman, M. A., & Cameselle, C. (2006). Improvement in electrokinetic remediation of heavy metal spiked kaolin with the polarity exchange technique. *Chemosphere, 62*(5), 817–822.

Pedersen, K. B., Lejon, T., Jensen, P. E., & Ottosen, L. M. (2016). Degradation of oil products in a soil from a Russian Barents hotspot during electrodialytic remediation. *SpringerPlus, 5*(1), 168.

Pham, T. D., Shrestha, R. A., Virkutyte, J., & Sillanp, M. (2009). Combined ultrasonication and electrokinetic remediation for persistent organic removal from contaminated kaolin. *Electrochimica Acta, 54*(5), 1403–1407.

Probstein, R. F., & Hicks, R. E. (1993). Removal of contaminants from soils by electric fields. *Science, 260*(5107), 498–503.

Reddy, K. R. (2010). Technical challenges to in-situ remediation of polluted sites. *Geotechnical and Geological Engineering, 28*(3), 211–221.

Reddy, K. R., & Saichek, R. E. (2003). Effect of soil type on electrokinetic removal of phenanthrene using surfactants and cosolvents. *Journal of Environmental Engineering, 129*(4), 336–346.

Ricart, M. T., Pazos, M., Gouveia, S., Cameselle, C., & Sanroman, M. A. (2008). Removal of organic pollutants and heavy metals in soils by electrokinetic remediation. *Journal of Environmental Science and Health, 43*(8), 871–875.

Rodríguez-Maroto, J. M., & Vereda-Alonso, C. (2009). Electrokinetic modeling of heavy metals. *Electrochemical Remediation Technologies for Polluted Soils, Sediments and Groundwater*, 537–562. https://doi.org/10.1002/9780470523650.ch25.

Rojo, A., Hansen, H. K., & Cubillos, M. (2012). Electrokinetic remediation using pulsed sinusoidal electric field. *Electrochimica Acta, 86*, 124–129.

Ryu, B. G., Yang, J. S., Kim, D. H., & Baek, K. (2010). Pulsed electrokinetic removal of Cd and Zn from fine-grained soil. *Journal of Applied Electrochemistry, 40*(6), 1039–1047.

Sarwar, N., Imran, M., Shaheen, M. R., Ishaque, W., Kamran, M. A., Matloob, A., Rehim, A., & Hussain, S. (2017). Phytoremediation strategies for soils contaminated with heavy metals: modifications and future perspectives. *Chemosphere, 171*, 710–721.

Shen, Z., Chen, X., Jia, J., Qu, L., & Wang, W. (2007). Comparison of electrokinetic soil remediation methods using one fixed anode and approaching anodes. *Environmental Pollution, 150*(2), 193–199.

Sprocati, R., & Rolle, M. (2020). Charge interactions, reaction kinetics and dimensionality effects on electrokinetic remediation: a model-based analysis. *Journal of Contaminant Hydrology, 229*, 103567.

Sprocati, R., Masi, M., Muniruzzaman, M., & Rolle, M. (2019). Modeling electrokinetic transport and biogeochemical reactions in porous media: a multidimensional Nernst–Planck–Poisson approach with PHREEQC coupling. *Advances in Water Resources, 127*, 134–147.

Sun, Y., Gao, K., Zhang, Y., & Zou, H. (2017). Remediation of persistent organic pollutant-contaminated soil using biosurfactant-enhanced electrokinetics coupled with a zero-valent iron/activated carbon permeable reactive barrier. *Environmental Science & Pollution Research, 24*(36), 28142–28151.

Sun, Z., Wu, B., Guo, P., Wang, S., & Guo, S. (2019). Enhanced electrokinetic remediation and simulation of cadmium-contaminated soil by superimposed electric field. *Chemosphere, 233*, 17–24.

Tang, X., Li, Q., Wang, Z., Hu, Y., Hu, Y., & Li, R. (2017). In situ electrokinetic isolation of cadmium from paddy soil through pore water drainage: effects of voltage gradient and soil moisture. *Chemical Engineering Journal, 337*, 210–219.

Tang, X., Li, Q., Wang, Z., Hu, Y., Hu, Y., & Scholz, M. (2018). Improved isolation of cadmium from paddy soil by novel technology based on pore water drainage with graphite-contained electro-kinetic geosynthetics. *Environmental Science & Pollution Research, 25*(14), 14244–14253.

Tang, X., Li, R., Han, D., & Wu, X. (2020). Impacts of electrokinetic isolation of phosphorus through pore water drainage on sediment phosphorus storage dynamics. *Environmental Pollution, 266*(Part 2), 115210.

Tang, J., Qiu, Z., Tang, H., Wang, H., Sima, W., Liang, C., Liao, Y., Li, Z., Wan, S., & Dong, J. (2021). Coupled with EDDS and approaching anode technique enhanced electrokinetic remediation remove heavy metal from sludge. *Environmental Pollution, 272*, 115975.

Vocciante, M., Bagatin, R., & Ferro, S. (2017). Enhancements in electrokinetic remediation technology: focus on water management and wastewater recovery. *Chemical Engineering Journal, 309*, 708–716.

Wang, Y., Li, A., & Cui, H. (2021). Remediation of heavy metal-contaminated soils by electrokinetic technology: mechanisms and applicability. *Chemosphere, 265*, 129071.

Wu, C., Yao, Y., & Xie, Q. (2013). Synergy remediation of PBDEs contaminated soil by electric — magnetic method. *Advanced Materials Research, 726*, 2338–2341.

Wu, J., Wei, B., Lv, Z., & Fu, Y. (2021). To improve the performance of focusing phenomenon related to energy consumption and removal efficiency in electrokinetic remediation of Cr-contaminated soil. *Separation and Purification Technology*, 118882.

Xiao, J., Zhou, S., Chu, L., & Liu, Y. (2020). Electrokinetic remediation of uranium(VI)-contaminated red soil using composite electrolyte of citric acid and ferric chloride. *Environmental Science and Pollution Research, 27*, 4478–4488.

Xie, Q., & Ma, X. (2018). Magnetic force-assisted electrokinetic remediation of triclosan-contaminated soil. *Journal of Jiangsu University (Natural Science), 39*(1), 92–95 (in Mandarin).

Xue, Z., Tang, X., & Yang, Q. (2017). Influence of voltage and temperature on electro-osmosis experiments applied on marine clay. *Applied Clay Science, 141*, 13–22.

Zhou, D. M., Alshawabkeh, A. N., Deng, C. F., Cang, L., & Si, Y. B. (2004). Electrokinetic removal of chromium and copper from contaminated soils by lactic acid enhancement in the catholyte. *Journal of Environmental Sciences, 16*(4), 529–532.

Zhou, A. X., Chen, N., Lu, J. Y., Fang, F., & Guo, J. S. (2011). Analysis and evaluation of sediment pollutant of secondary rivers of the three gorges reservoir. *Procedia Environmental Sciences, 10*, 2147–2152.

Zhou, M., Zhu, S., Liu, Y., & Wang, H. (2014). Electrokinetic remediation of fluorine-contaminated soil using approaching cathodes. *CLEAN – Soil, Air, Water, 42*(12), 1771–1775.

Zhou, M., Wang, H., Zhu, S., Liu, Y., & Xu, J. (2015). Electrokinetic remediation of fluorine-contaminated soil and its impact on soil fertility. *Environmental Science & Pollution Research, 22*(21), 16907–16913.

Zhu, S., Zhang, J., & Dong, T. (2009). Removal of fluorine from contaminated field soil by anolyte enhanced electrokinetic remediation. *Environmental Earth Sciences, 59*, 379–384.